monkeys. CT, normal adult monkeys; DM, DM-affected adult monkeys. (G) Age-related and DM-related changes in APP, Rab5, Rab7, and Rab11 in cynomolgus monkey brains. Data obtained from young monkey brains were set as standards; *P<0.05 **P<0.01. Y-axes show the mean values of the quantified data. Y, young monkeys; CT, normal adult monkeys; DM, DM-affected adult monkeys; AG, normal aged monkeys.

doi:10.1371/journal.pone.0117362.g005

studies are needed, these findings suggest that DM can induce not only parenchymal Aβ pathology but also vascular Aβ pathology in an age-dependent manner.

To clarify the mechanism of how DM enhances Aβ pathology in the brain, we also assessed the amount of Aβ and GAβ, a seed molecule for Aβ aggregation [32]. Intriguingly, Aβ level was not so much increased in DM-affected adult monkey brains, in contrast to aged monkey brains (Fig. 4A). In DM-affected adult monkey brains, SP depositions were quite small quantities (Fig. 2I), and a couple of more years can induce age-dependent SP depositions in normal adult monkey brains [26, 36]. That may be why we could not find the significant increase of Aβ level between DM-affected adult monkey and normal adult monkey brains. On the other hand, both immunohistochemical and dot blot analyses demonstrated that the amount of GAβ was clearly increased in the brains of DM-affected adult monkeys compared to control adult monkey brains (Fig. 4B-E). These findings strongly suggest that the acceleration of GAβ generation might be responsible for the early deposition of SPs in the brains of DM-affected adult

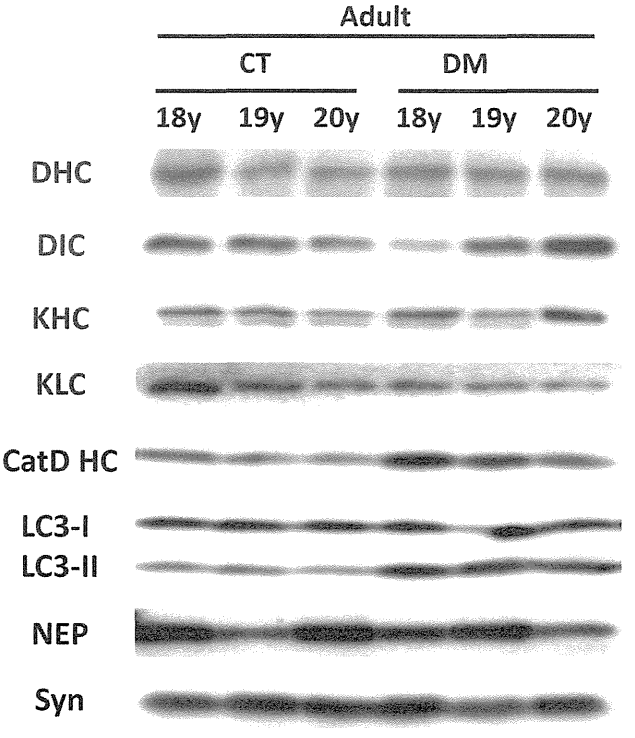

Fig 6. Western blot analyses of axonal motor proteins, cathepsin D heavy chain, autophagosome marker LC3, and neprilysin in the brains of normal and DM-affected adult monkeys. Western blots showing the amounts of axonal motor proteins, cathepsin D heavy chain (CatD HC), autophagosome marker LC3, and neprilysin (NEP) in the brains of normal and DM-affected adult monkeys. Western blot analyses showed that the level of axonal motor proteins such as dynein heavy chain (DHC), dynein intermediate chain (DIC), kinesin heavy chain (KHC), and kinesin light chain (KLC) unchanged. The level of CatD HC increased in DM-affected monkey brains, and LC3-II showed significant increase in DM-affected adult monkeys. We did not observed DM-related changes in LC3-I and neprilysin (NEP) level. CT, normal adult monkeys; DM, DM-affected adult monkeys.

doi:10.1371/journal.pone.0117362.g006

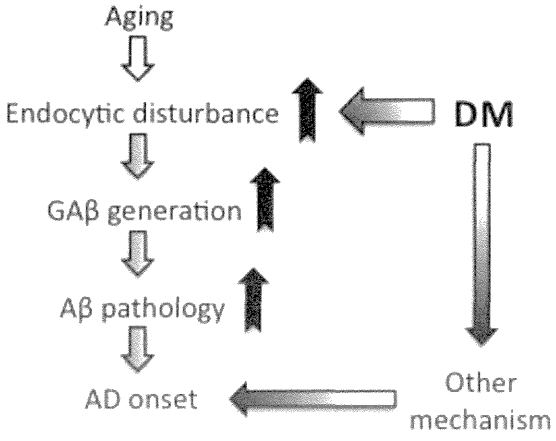

Fig 7. Hypothetical schema of DM-induced Aβ pathology leading to AD onset. From the results of this study, we propose that DM induces GAβ generation by exacerbating age-dependent endocytic disturbance, resulting in enhanced Aβ pathology in the brain. Although additional studies are needed to clarify the whole mechanisms underlying DM-associated pathology, we hypothesize that, at the very least, enhanced Aβ pathology accompanied by endocytic disturbance might be involved in the development of AD.

doi:10.1371/journal.pone.0117362.g007

monkeys. Moreover, the result of this study also suggests that enhanced Aβ aggregation could induce SP deposition without significant changes in total Aβ level. Relevant to proposed AD pathophysiogical mechanisms, we also observed apparent endocytic pathology, including enlarged early endosomes and APP accumulation in neurons of DM-affected adult monkeys (Fig. 5A-E). Western blot analyses confirmed a significant increase of Rab GTPases in these brains at nearly the same level as in aged monkey brains (Fig. 5F, G). Our previous studies showed that an increase in Rab GTPases is a good indicator for alterations in intracellular endosome trafficking associated with a particular Rab GTPase [45, 46]. Indeed, increased Rab GTPase levels are strongly associated with endocytic disturbance [45, 46]. The observation that experimentally induced disorders of the endocytic pathway cause GAβ-dependent Aβ pathology [34, 52] supports the premise that endocytic disturbance is likely responsible for enhanced GAβ generation. Along these lines, we surmise that intracellular endosome trafficking would be altered in the brains of DM-affected adult monkeys, resulting in severe endocytic disturbance, as observed in aged monkey brains. This might be why GAβ generation was enhanced, thereby inducing SP deposition (Fig. 2). Moreover, the results of this study strongly support the idea that endocytic disturbance is essentially involved in the development of AD pathology [33, 34, 42–45].

A recent study showed that the expression of axonal transport motor proteins was altered in experimentally DM-induced rodent model, and axonal transport motor proteins are indeed required for endosome trafficking [48, 49]. However, in the present study, we did not find any changes in axonal motor protein levels, suggesting that the mechanism underlying endocytic disturbance in the brains of DM-affected adult monkeys would be independent of axonal motor protein levels. Previous finding showed that the breakdown in lysosomal degradation also induces endocytic disturbance [50]. In DM-affected adult monkey brains, the level of CatD heavy chain increased in DM-affected adult monkey brains, indicating that the endosomal-lysosomal system is activated as such in AD patient brains (Fig. 6) [53]. This finding suggests that DM really enhances AD pathology. On the other hand, we observed the significant increase in autophagosome marker LC3-II level in DM-affected adult monkey brains (Fig. 6). Since LC3-I level was unchanged, the induction of autophagy was not altered, but lysosomal-

autophagosome clearance was likely disturbed in DM-affected adult monkey brains (Fig. 6). The defective lysosomal-autophagosome clearance is associated with AD pathology [50, 54–56], and the result of this study is also consistent with a previous finding that the aberrant lysosomal-autophagic turnover is associated with the accumulation of GAβ in rodent brain [57].

Given that CatD heavy chain level was increased, i.e. lysosomal degradation was induced (Fig. 6), the disturbance in the fusion of autophagosome and lysosome might be responsible for impaired lysosomal-autophagosome clearance in DM-affected adult monkey brains. The fusion step is indispensable for lysosomal-autophagosome clearance [58, 59] and mediated by Rab7 [60]. In DM-affected adult monkey brains, Rab7 level was obviously increased as compared to normal adult monkey brains, indicating that Rab7-mediated transport was really disturbed. Growing evidences suggest that membrane-bound phosphoinositides regulate Rab-mediated endosome trafficking [61, 62], and the metabolism of phosphoinositides was affected by the disruption of insulin signaling [63–65]. Recent studies also showed that Rab activity is affected by insulin signaling and that PI3K inhibition causes upregulation of Rab5 [66, 67]. In the present study, we observed amyloid deposition in the pancreatic islets of all adult monkeys with DM. The remaining islet cells were severely degenerated and few in number, all characteristics of DM pathology in humans. These pancreatic pathologies suggest that insulin signaling also would be greatly impaired in the brains of DM-affected adult monkeys (Fig. 1A-D). Thus, although additional investigations are needed, impaired insulin signaling would exacerbate age-related endocytic disturbances via such alteration in the metabolism of phosphoinositides and/or Rab GTPases, inducing GAβ generation and ultimately resulting in enhanced Aβ pathology. It is reasonable idea because of the fact that insulin resistance is the core defect in DM [68]. In the brains of DM-affected adult monkeys, NEP levels were not affected (Fig. 6), suggesting that the enhanced SP deposition we observed is not due to disturbances in Aβ degradation by NEP.

In conclusion, we provide evidence that DM induces GAβ generation and accelerates Aβ pathology *in vivo* in cynomolgus monkey brains. Since the amino acid sequence of cynomolgus monkey Aβ corresponds completely with that of human Aβ, it is reasonable that the enhanced Aβ pathology we observed in monkeys with DM should also occur in humans with DM. Moreover, our present study showed that DM could also exacerbate endocytic disturbance. Although additional studies are needed to determine more precisely the mechanisms responsible for enhanced Aβ pathology in the brains of DM-affected monkeys, our findings suggest that DM may exacerbate age-dependent endocytic disturbance, leading to enhanced GAβ generation and Aβ fibril formation (Fig. 7). Importantly, several studies showed that Aβ impairs insulin signaling itself [69–71], and then it may lead to aggravate the insulin resistance-related AD pathology [11–13]. Thus enhanced Aβ pathology would contribute to DM-induced AD pathogenesis with such other mechanism (Fig. 7). Moreover, DM may also alter neuronal activity by exacerbating endocytic disturbance as we previously reported [46]. Hence, a reasonable therapeutic strategy to prevent the development of AD pathology is to treat or prevent DM.

Supporting Information

S1 ARRIVE Checklist. The ARRIVE Guidelines Checklist.
(PDF)

S1 Table. Clinical Background of monkeys analyzed in the present study.
(XLSX)

Acknowledgments

The authors thank Dr. Fumiko Ono for autopsy of cynomolgus monkeys. The authors also thank Dr. Naoto Oikawa for technical advice in dot blot analyses.

Author Contributions

Conceived and designed the experiments: NK. Performed the experiments: SO NK. Analyzed the data: SO NS YY KY NK. Contributed reagents/materials/analysis tools: NS YY. Wrote the paper: NK.

References

1. Armstrong RA (2009) The molecular biology of senile plaques and neurofibrillary tangles in Alzheimer's disease. Folia Neuropathol 47:289–299. PMID: 20054780
2. Mattson MP (2004) Pathways towards and away from Alzheimer's disease. Nature 430:631–639. PMID: 15295589
3. Hardy J, Selkoe DJ (2002) The amyloid hypothesis of Alzheimer's disease: progress and problems on the road to therapeutics. Science 297:353–356. PMID: 12130773
4. Goedert M, Sisodia SS, Price DL (1991) Neurofibrillary tangles and beta-amyloid deposits in Alzheimer's disease. Curr Opin Neurobiol 1:441–447. PMID: 1821689
5. Leibson CL, Rocca WA, Hanson VA, Cha R, Kokmen E, O'Brien PC, et al. (1997) Risk of dementia among persons with diabetes mellitus: a population-based cohort study. Am J Epidemiol 145:301–308. PMID: 9054233
6. Arvanitakis Z, Wilson RS, Bienias JL, Evans DA, Bennett DA (2004) Diabetes mellitus and risk of Alzheimer disease and decline in cognitive function. Arch Neurol 61:661–666. PMID: 15148141
7. Frisardi V, Solfrizzi V, Seripa D, Capurso C, Santamato A, et al. (2010) Metabolic-cognitive syndrome: a cross-talk between metabolic syndrome and Alzheimer's disease. Ageing Res Rev 9:399–417. doi: 10.1016/j.arr.2010.04.007 PMID: 20444434
8. Daviglus ML, Plassman BL, Pirzada A, Bell CC, Bowen PE, et al. (2011) Risk factors and preventive interventions for Alzheimer disease: state of the science. Arch Neurol 68:1185–1190. doi: 10.1001/archneurol.2011.100 PMID: 21555601
9. Crane PK, Walker R, Hubbard RA, Li G, Nathan DM, Zheng H, et al. (2013) Glucose levels and risk of dementia. N Engl J Med 369:540–548. doi: 10.1056/NEJMoa1215740 PMID: 23924004
10. Ott A, Stolk RP, van Harskamp F, Pols HAP, Hofman A, et al. (1999) Diabetes mellitus and the risk of dementia: the Rotterdam Study. Neurology 53:1937–1942. PMID: 10599761
11. De Felice FG, Ferreira ST (2014) Inflammation, defective insulin signaling, and mitochondrial dysfunction as common molecular denominators connecting type 2 diabetes to Alzheimer disease. Diabetes 63:2262–72. doi: 10.2337/db13-1954 PMID: 24931033
12. Salkovic-Petrisic M, Tribl F, Schmidt M, Hoyer S, Riederer P (2006) Alzheimer-like changes in protein kinase B and glycogen synthase kinase-3 in rat frontal cortex and hippocampus after damage to the insulin signalling pathway. J Neurochem 96:1005–15. PMID: 16412093
13. Baker LD, Cross DJ, Minoshima S, Belongia D, Watson GS, et al. (2010) Insulin resistance and Alzheimer-like reductions in regional cerebral glucose metabolism for cognitively normal adults with prediabetes or early type 2 diabetes. Arch Neurol 68:51–7. doi: 10.1001/archneurol.2010.225 PMID: 20837822
14. Ho L, Qin W, Pompl PN, Xiang Z, Wang J, et al. (2004) Diet-induced insulin resistance promotes amyloidosis in a transgenic mouse model of Alzheimer's disease. FASEB J 18:902–4. PMID: 15033922
15. Li Y, Duffy KB, Ottinger MA, Ray B, Bailey JA, et al. (2010) GLP-1 receptor stimulation reduces amyloid-beta peptide accumulation and cytotoxicity in cellular and animal models of Alzheimer's disease. J Alzheimers Dis 19:1205–19. doi: 10.3233/JAD-2010-1314 PMID: 20308787
16. Plaschke K, Kopitz J, Siegelin M, Schliebs R, Salkovic-Petrisic M, et al. (2010) Insulin-resistant brain state after intracerebroventricular streptozotocin injection exacerbates Alzheimer-like changes in Tg2576 AbetaPP-overexpressing mice. J Alzheimers Dis 19:691–704. doi: 10.3233/JAD-2010-1270 PMID: 20110613
17. Takeda S, Sato N, Uchio-Yamada K, Sawada K, Kunieda T, et al. (2010) Diabetes-accelerated memory dysfunction via cerebrovascular inflammation and Aβ deposition in an Alzheimer mouse model with diabetes. Proc Natl Acad Sci USA 107:7036–7041. doi: 10.1073/pnas.1000645107 PMID: 20231468

18. Bitela CL, Kasinathanb C, Kaswalab RH, Klein WL, Frederiksea PH (2012) Amyloid-β and Tau Pathology of Alzheimer's Disease Induced by Diabetes in a Rabbit Animal Model. Journal of Alzheimer's Disease 32:291–305. doi: 10.1111/tra.12264 PMID: 25615530

19. Currais A, Prior M, Lo D, Jolivalt C, Schubert D, et al. (2012) Diabetes exacerbates amyloid and neurovascular pathology in aging-accelerated mice. Aging Cell 11:1017–26. doi: 10.1111/acel.12002 PMID: 22938075

20. Maesako M, Uemura K, Kubota M, Kuzuya A, Sasaki K, et al. (2012) Environmental enrichment ameliorated high-fat diet-induced Aβ deposition and memory deficit in APP transgenic mice. Neurobiol Aging 33:1011.e11–23.

21. Son SM, Song H, Byun J, Park KS, Jang HC, et al. (2012) Accumulation of autophagosomes contributes to enhanced amyloidogenic APP processing under insulin-resistant conditions. Autophagy 8:1842–4. doi: 10.4161/auto.21861 PMID: 22931791

22. Yamamoto N, Matsubara T, Sobue K, Tanida M, Kasahara R, et al. (2012) Brain insulin resistance accelerates Aβ fibrillogenesis by inducing GM1 ganglioside clustering in the presynaptic membranes. J Neurochem 121:619–28. doi: 10.1111/j.1471-4159.2012.07668.x PMID: 22260232

23. Chen Y, Liang Z, Blanchard J, Dai CL, Sun S, et al. (2013) A non-transgenic mouse model (icv-STZ mouse) of Alzheimer's disease: similarities to and differences from the transgenic model (3xTg-AD mouse). Mol Neurobiol 47:711–25. doi: 10.1007/s12035-012-8375-5 PMID: 23150171

24. Yang Y, Wu Y, Zhang S, Song W (2013) High glucose promotes Aβ production by inhibiting APP degradation. PLoS One 8:e69824. doi: 10.1371/journal.pone.0069824 PMID: 23894546

25. Mehlaa J, Chauhanc BC, Chauhana NB (2014) Experimental Induction of Type 2 Diabetes in Aging-Accelerated Mice Triggered Alzheimer-Like Pathology and Memory Deficits. J Alzheimers Dis 39:145–162. doi: 10.3233/JAD-131238 PMID: 24121970

26. Nakamura S, Nakayama H, Goto N, Sakakibara I, Yosikawa Y (1998) Histopathological studies of senile plaques and cerebral amyloidosis in cynomolgus monkeys. J Med Primatol 27:244–252. PMID: 9926980

27. Oikawa N, Kimura N, Yanagisawa K (2010) Alzheimer-type tau pathology in advanced aged nonhuman primate brains harboring substantial amyloid deposition. Brain Res 1315:137–149. doi: 10.1016/j.brainres.2009.12.005 PMID: 20004650

28. Podlisny MB, Tolan DR, Selkoe DJ (1991) Homology of the amyloid beta protein precursor in monkey and human supports a primate model for beta amyloidosis in Alzheimer's disease. Am J Pathol 138:1423–1435. PMID: 1905108

29. Wagner JD, Cline JM, Shadoan MK, Bullock BC, Rankin SE, et al. (2001) Naturally occurring and experimental diabetes in cynomolgus monkeys: a comparison of carbohydrate and lipid metabolism and islet pathology. Toxicol Pathol 29: 142–148. PMID: 11215678

30. Wagner JE, Kavanagh K, Ward GM, Auerbach BJ, Harwood HJ Jr, et al. (2006) Old world nonhuman primate models of type 2 diabetes mellitus. ILAR J 47:259–271. PMID: 16804200

31. Bauer SA, Arndt TP, Leslie KE, Peral DL, Turner PV (2011) Obesity in rhesus and cynomolgus macaques: a comparative review of the condition and its implications for research. Comp Med 61:541–526.

32. Yanagisawa K, Odaka A, Suzuki N, Ihara Y (1995) GM1 ganglioside-bound amyloid beta-protein (A beta): a possible form of preamyloid in Alzheimer's disease. Nature Med 1:1062–1066. PMID: 7489364

33. Kimura N, Yanagisawa K (2007) Endosomal accumulation of GM1 ganglioside-bound amyloid beta-protein in neurons of aged monkey brains. Neuroreport 18:1669–1673. PMID: 17921865

34. Yuyama K, Yamamoto N, Yanagisawa K (2006) Chloroquine-induced endocytic pathway abnormalities: Cellular model of GM1 ganglioside-induced Abeta fibrillogenesis in Alzheimer's disease. FEBS Lett 580:6972–6976. PMID: 17161396

35. Tsuchida J, Yoshida T, Sankai T, Yasutomi Y (2008) Maternal behavior of laboratory-born, individually reared long-tailed macaques (Macaca fascicularis). J Am Assoc Lab Anim Sci 47:29–34. PMID: 18947167

36. Kimura N, Yanagisawa K, Terao K, Ono F, Sakakibara I, et al. (2005) Age-related changes of intracellular Abeta in cynomolgus monkey brains. Neuropathol Appl Neurobiol 31:170–180. PMID: 15771710

37. MacLaurin J, Chakrabartty A (1996) Membrane disruption by Alzheimer β-amyloid peptides mediated through specific binding to either phospholipids or gangliosides. Implications for neurotoxicity. J Biol Chem 271:26482–26489. PMID: 8900116

38. Choo-Smith LP, Garzon-Rodriguez W, Glabe CG, Surewicz WK (1997) Acceleration of amyloid fibril formation by specific binding of Abeta-(1–40) peptide to ganglioside-containing membrane vesicles. J Biol Chem 272:22987–22990. PMID: 9287293

39. Matsusaki K, Horikiri C (1999) Interactions of amyloid beta-peptide (1–40) with ganglioside-containing membranes. Biochemistry 38:4137–4142. PMID: 10194329

40. Kakio A, Nishimoto S, Yanagisawa K, Kozutsumi Y, Matsuzaki K (2002) Interactions of amyloid beta-protein with various gangliosides in raft-like membranes: importance of GM1 ganglioside-bound form as an endogenous seed for Alzheimer amyloid. Biochemistry 41:4385–7390. PMID: 11914085

41. Hayashi H, Kimura N, Yamaguchi H, Hasegawa K, Yokoseki T, et al. (2004) A seed for Alzheimer amyloid in the brain. J Neurosci 24:4894–4902. PMID: 15152051

42. Cataldo AM, Barnett JL, Pieroni C, Nixon RA (1997) Increased neuronal endocytosis and protease delivery to early endosomes in sporadic Alzheimer's disease: neuropathologic evidence for a mechanism of increased beta-amyloidogenesis. J Neurosci 17:6142–6151. PMID: 9236226

43. Cataldo AM, Peterhoff CM, Troncoso JC, Gomez-Isla T, Hyman BT, et al. (2000) Endocytic pathway abnormalities precede amyloid beta deposition in sporadic Alzheimer's disease and Down syndrome: differential effects of APOE genotype and presenilin mutations. Am J Pathol 157:277–286. PMID: 10880397

44. Cataldo AM, Petanceska S, Terio NB, Peterhoff CM, Durham R, et al. (2004) Abeta localization in abnormal endosomes: association with earliest Abeta elevations in AD a syndrome. Neurobiol Aging 25:1263–1272. PMID: 15465622

45. Kimura N, Inoue M, Okabayashi S, Ono F, Negishi T (2009) Dynein dysfunction induces endocytic pathology accompanied by an increase in Rab GTPases: a potential mechanism underlying age-dependent endocytic dysfunction. J Biol Chem 284:31291–31302. doi: 10.1074/jbc.M109.012625 PMID: 19758999

46. Kimura N, Okabayashi S, Ono F (2012) Dynein dysfunction disrupts intracellular vesicle trafficking bidirectionally and perturbs synaptic vesicle docking via endocytic disturbances a potential mechanism underlying age-dependent impairment of cognitive function. Am J Pathol 180:550–561. doi: 10.1016/j.ajpath.2011.10.037 PMID: 22182700

47. Kimura N, Tanemura K, Nakamura S, Takashima A, Ono F, et al. (2003) Age-related changes of Alzheimer's disease-associated proteins in cynomolgus monkey brains. Biochem Biophys Res Comm 310:303–311. PMID: 14521910

48. Schroer TA, Sheetz MP (1991) Functions of microtubule-based motors. Annu Rev Physiol 53:629–52. PMID: 2042975

49. Baptista FI, Pinto MJ, Elvas F, Almeida RD, Ambrósio AF (2013) Diabetes Alters KIF1A and KIF5B Motor Proteins in the Hippocampus. PLOS ONE 8:e65515. doi: 10.1371/journal.pone.0065515 PMID: 23776493

50. Nixon RA, Cataldo AM, Mathews PM (2000) The endosomal-lysosomal system of neurons in Alzheimer's disease pathogenesis: a review. Neurochem Res 25:1161–72. PMID: 11059790

51. Liu Y, Liu L, Lu S, Wang D, Liu X, et al. (2011) Impaired amyloid β-degrading enzymes in brain of streptozotocin-induced diabetic rat. J Endocrinol Invest 34:26–31. doi: 10.3275/6995 PMID: 20414044

52. Yuyama K, Yanagisawa K (2009) Late endocytic dysfunction as a putative cause of amyloid fibril formation in Alzheimer's disease. J Neurochem 109:1250–1260. doi: 10.1111/j.1471-4159.2009.06046.x PMID: 19317854

53. Cataldo AM, Barnett JL, Berman SA, Li J, Quarless S, et al. (1995) Gene expression and cellular content of cathepsin D in Alzheimer's disease brain: evidence for early up-regulation of the endosomal-lysosomal system. Neuron 14: 671–80. PMID: 7695914

54. Nixon RA, Wegiel J, Kumar A, Yu WH, Peterhoff C, et al. (2005) Extensive involvement of autophagy in Alzheimer disease: an immuno-electron microscopy study. J Neuropathol Exp Neurol 64: 113–22. PMID: 15751225

55. Boland B, Kumar A, Lee S, Platt FM, Wegiel J, et al. (2008) Autophagy induction and autophagosome clearance in neurons: relationship to autophagic pathology in Alzheimer's disease. J Neurosci 28: 6926–37. doi: 10.1523/JNEUROSCI.0800-08.2008 PMID: 18596167

56. Wolfe DM, Lee JH, Kumar A, Lee S, Orenstein SJ, et al. (2013) Autophagy failure in Alzheimer's disease and the role of defective lysosomal acidification. Eur J Neurosci 37: 1949–61. doi: 10.1111/ejn.12169 PMID: 23773064

57. Keilani S, Lun Y, Stevens AC, Williams HN, Sjoberg ER, et al. (2012) Lysosomal dysfunction in a mouse model of Sandhoff disease leads to accumulation of ganglioside-bound amyloid-β peptide. J Neurosci 32: 5223–36. doi: 10.1523/JNEUROSCI.4860-11.2012 PMID: 22496568

58. Tooze J, Hollinshead M, Ludwig T, Howell K, Hoflack B, et al. (1990) In exocrine pancreas, the basolateral endocytic pathway converges with the autophagic pathway immediately after the early endosome. J Cell Biol 111: 329–45. PMID: 2166050

59. Berg TO, Fengsrud M, Strømhaug PE, Berg T, Seglen PO (1998) Isolation and characterization of rat liver amphisomes. Evidence for fusion of autophagosomes with both early and late endosomes. J Biol Chem 273: 21883–92. PMID: 9705327

60. Gutierrez MG, Munafó DB, Berón W, Colombo MI (2004) Rab7 is required for the normal progression of the autophagic pathway in mammalian cells J Cell Sci 117: 2687–97. PMID: 15138286

61. Falkenburger BH, Jensen JB, Dickson EJ, Suh BC, Hille B (2010) Phosphoinositides: lipid regulators of membrane proteins. J Physiol 588: 3179–3185. doi: 10.1113/jphysiol.2010.192153 PMID: 20519312

62. Zhang X, Li X, Xu H (2012) Phosphoinositide isoforms determine compartment-specific ion channel activity. Proc Natl Acad Sci U S A 109: 11384–11389. doi: 10.1073/pnas.1202194109 PMID: 22733759

63. Natarajan V, Dyck PJ, Schmid HH (1981) Alterations of inositol lipid metabolism of rat sciatic nerve in streptozotocin-induced diabetes. J Neurochem 36: 413–9. PMID: 7463069

64. Thakker JK, DiMarchi R, MacDonald K, Caro JF (1989) Effect of Insulin and Insulin-like Growth Factors I and II on Phosphatidylinositol and Phosphatidylinositol 4,5-Bisphosphate Breakdown in Liver from Humans With and Without Type II Diabetes. J Biol Chem 264: 7169–7175. PMID: 2540178

65. Kamada T, McMillan DE, Otsuji S (1992) Changes in polyphosphoinositides and phosphatidic acid of erythrocyte membranes in diabetes. Diabetes Res Clin Pract 16: 85–90. PMID: 1318189

66. Huang J, Imamura T, Olefsky JM (2001) Insulin can regulate GLUT4 internalization by signaling to Rab5 and the motor protein dynein. Proc Natl Acad Sci USA 98:13084–13089. PMID: 11687655

67. Runyan CE, Liu Z, Schnaper HW (2012) Phosphatidylinositol 3-kinase and Rab5 GTPase inversely regulate the Smad anchor for receptor activation (SARA) protein independently of transforming growth factor-β1. J Biol Chem 287:35815–35824. doi: 10.1074/jbc.M112.380493 PMID: 22942286

68. Goldstein BJ (2002) Insulin resistance as the core defect in type 2 diabetes mellitus. Am J Cardiol 90:3G–10G. PMID: 12231073

69. Zhao WQ, De Felice FG, Fernandez S, Chen H, Lambert MP, et al. (2008) Amyloid beta oligomers induce impairment of neuronal insulin receptors. FASEB J 22:246–60. PMID: 17720802

70. De Felice FG, Vieira MN, Bomfim TR, Decker H, Velasco PT, et al. (2009) Protection of synapses against Alzheimer's-linked toxins: insulin signaling prevents the pathogenic binding of Abeta oligomers. Proc Natl Acad Sci U S A 106:1971–6. doi: 10.1073/pnas.0809158106 PMID: 19188609

71. Bomfim TR, Forny-Germano L, Sathler LB, Brito-Moreira J, Houzel JC, et al. (2012) An anti-diabetes agent protects the mouse brain from defective insulin signaling caused by Alzheimer's disease- associated Aβ oligomers. J Clin Invest 122:1339–53. doi: 10.1172/JCI57256 PMID: 22476196

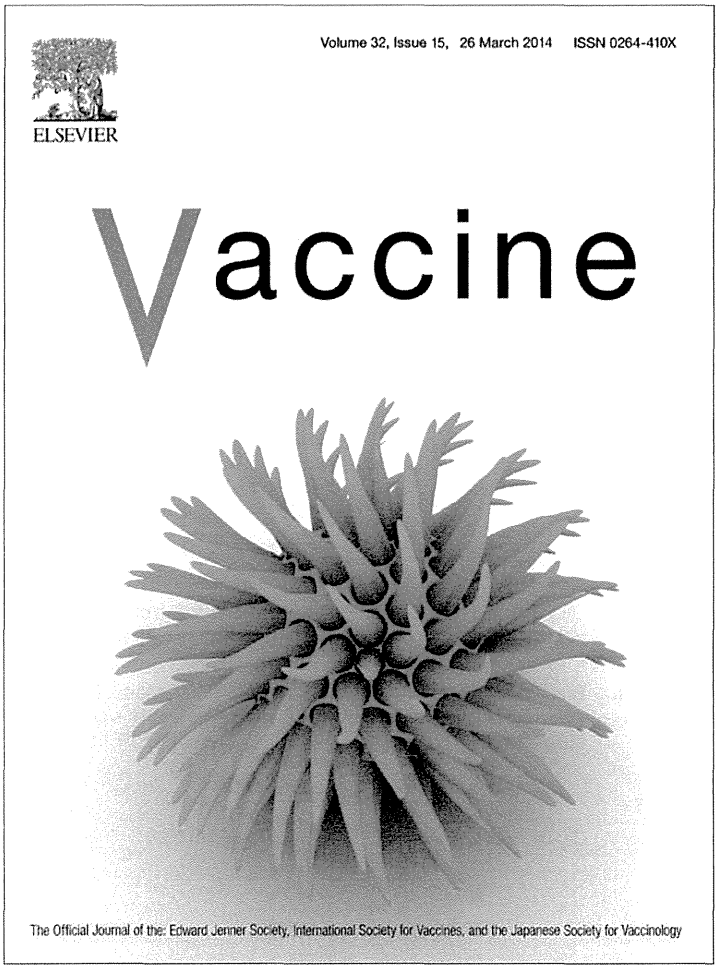

Vaccine 32 (2014) 1727–1735

Contents lists available at ScienceDirect

Vaccine

journal homepage: www.elsevier.com/locate/vaccine

Recombinant Ag85B vaccine by taking advantage of characteristics of human parainfluenza type 2 virus vector showed Mycobacteria-specific immune responses by intranasal immunization

Kenta Watanabe[a,1], Akihiro Matsubara[a,b,1], Mitsuo Kawano[c], Satoru Mizuno[d,e], Tomotaka Okamura[a], Yusuke Tsujimura[a], Hiroyasu Inada[f], Tetsuya Nosaka[c], Kazuhiro Matsuo[d], Yasuhiro Yasutomi[a,b,*]

[a] Laboratory of Immunoregulation and Vaccine Research, Tsukuba Primate Research Center, National Institute of Biomedical Innovation, Tsukuba, Ibaraki 305-0843, Japan
[b] Division of Immunoregulation, Department of Molecular and Experimental Medicine, Mie University Graduate School of Medicine, Tsu, Mie 514-8507, Japan
[c] Department of Microbiology and Molecular Genetics, Mie University Graduate School of Medicine, Tsu, Mie 514-8507, Japan
[d] Research and Development Department, Japan BCG Laboratory, Kiyose, Tokyo 204-0022, Japan
[e] The Research Institute of Tuberculosis, Kiyose, Tokyo 204-8533, Japan
[f] Department of Pathology, Faculty of Pharmaceutical Science, Suzuka University of Medical Science, Suzuka, Mie 513-8670, Japan

ARTICLE INFO

Article history:
Received 24 May 2013
Received in revised form
25 November 2013
Accepted 29 November 2013
Available online 29 January 2014

Keywords:
Human parainfluenza virus
Ag85B
Tuberculosis
Mucosal immunity

ABSTRACT

Viral vectors are promising vaccine candidates for eliciting suitable Ag-specific immune response. Since *Mycobacterium tuberculosis* (Mtb) normally enters hosts *via* the mucosal surface of the lung, the best defense against Mtb is mucosal vaccines that are capable of inducing both systemic and mucosal immunity. Although *Mycobacterium bovis* bacille Calmette-Guérin is the only licensed tuberculosis (TB) vaccine, its efficacy against adult pulmonary forms of TB is variable. In this study, we assessed the effectiveness of a novel mucosal TB vaccine using recombinant human parainfluenza type 2 virus (rhPIV2) as a vaccine vector in BALB/c mice. Replication-incompetent rhPIV2 (M gene-eliminated) expressing Ag85B (rhPIV2–Ag85B) was constructed by reverse genetics technology. Intranasal administration of rhPIV2–Ag85B induced Mtb-specific immune responses, and the vaccinated mice showed a substantial reduction in the number of CFU of Mtb in lungs and spleens. Unlike other viral vaccine vectors, the immune responses against Ag85B induced by rhPIV2–Ag85B immunization had an advantage over that against the viral vector. In addition, it was revealed that rhPIV2–Ag85B in itself has an adjuvant activity through the retinoic acid-inducible gene I receptor. These findings provide further evidence for the possibility of rhPIV2–Ag85B as a novel TB vaccine.

1. Introduction

Recombinant viral vector vaccines have several advantages for preventing infection with pathogens [1]. The vaccines induce a full spectrum of immune responses including humoral and cellular immune responses. These immune responses can be initially induced at the viral vector infection site such as mucosal immune responses [2]. Moreover, the viral vector itself has adjuvant activities through the innate immune systems [3]. Pre-existing or post-priming immune responses against the vaccine vector itself, however, could be an obstacle to effective immune responses to recombinant Ag [4]. Negligible immune responses against vector viruses compared with recombinant vaccine Ags after immunization is considered most desirable for recombinant viral vaccines.

Abbreviations: BAL, bronchoalveolar lavage; BCG, *Mycobacterium bovis* bacille Calmette-Guérin; BEAS cells, bronchial epithelial cells; hPIV2, human parainfluenza type 2 virus; pLN, pulmonary lymph node; Mtb, *Mycobacterium tuberculosis*; NHBE, normal human bronchial epithelial; rhPIV2–Ag85B, recombinant hPIV2 expressing Ag85B; TB, tuberculosis.

* Corresponding author at: Laboratory of Immunoregulation and Vaccine Research, Tsukuba Primate Research Center, National Institute of Biomedical Innovation, 1-1 Hachimandai, Tsukuba, Ibaraki 305-0843, Japan. Tel.: +81 29 837 2053; fax: +81 29 837 2053.
E-mail addresses: yasutomi@nibio.go.jp, yasutomi@doc.medic.mie-u.ac.jp (Y. Yasutomi).
[1] These authors contributed equally to this work.

0264-410X/$ – see front matter © 2014 Elsevier Ltd. All rights reserved.
http://dx.doi.org/10.1016/j.vaccine.2013.11.108

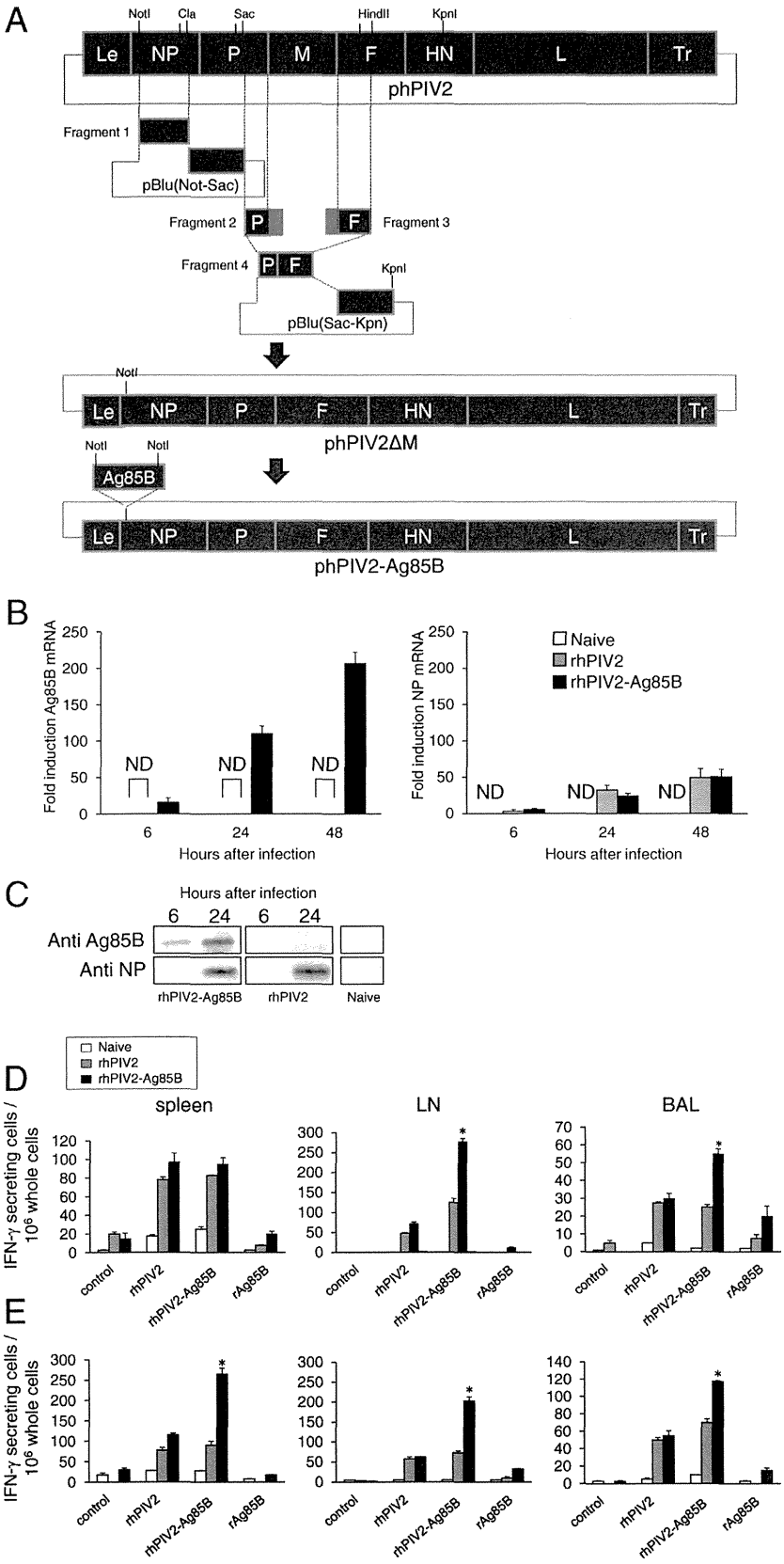

Fig. 1. Expression of Ag85B and advantageous effects in cellular immune response against Ag85B *versus* virus vector in immunized mice. (A) Construction of rhPIV2–Ag85B. (B) Expression of Ag85B (left panel) and NP (right panel) gene in BEAS cells infected with rhPIV2 or rhPIV2–Ag85B at each time point was determined by real-time PCR. Total RNA was extracted at 6, 24, and 48 h after infection. Fold increase of each target gene was normalized to β-actin, and the expression levels are represented as relative values to naïve cells. Error bars represent standard deviation. ND indicates non-detected. (C) Expression of Ag85B and NP proteins was detected by anti-Ag85B and anti-NP antibodies at 6 and 24 h after infection, respectively. (D and E) Mice were immunized 1 (D) or 2 (E) times with rhPIV2 or rhPIV2–Ag85B at a 2-week interval by intranasal

Mycobacterium bovis bacille Calmette-Guérin (BCG) has substantially contributed to the control of tuberculosis (TB) for more than 80 years and affords about 80% protection against tuberculosis meningitis and miliary tuberculosis in infant and young children. However, it is well known that the protective efficacy of BCG against pulmonary TB in adults is variable and partial [5,6]. Therefore, development of new vaccines is urgently needed for the elimination of TB as a public health threat and should be a major global public health priority.

Many infectious diseases, including TB, initially establish infection on mucosal surfaces. Therefore, the best defense against these predominantly mucosal pathogens is mucosal vaccines that are capable of inducing both systemic and mucosal immunity. However, the mucosal immune system is quite unique and is different from systemic immune responses [7,8]. Mucosal immunization provides mucosal immune responses in all mucosal effector tissues in the concept of a common mucosal immune system [9].

Human parainfluenza type 2 virus (hPIV2) is a member of the genus *Rubulavirus* of the family *Paramyxoviridae* and possesses a single-stranded, nonsegmented and negative-stranded RNA genome. This virus does not have a DNA phase during its life cycle and can avoid genetic modifications. Additionally, this virus becomes replication-incompetent by elimination of some viral genes [10]. Moreover, it is likely to lead to elicit stronger inserted antigen-specific immune responses than vector-specific responses unlike other viral vaccine vectors using inserted antigen expression mechanisms of hPIV2. In the present study, we evaluated the effectiveness of intranasal administration of Ag85B-expressed non-replicating human parainfluenza type 2 virus (rhPIV2–Ag85B), which induces weak immune responses against a viral vector, as a novel mucosal TB vaccine.

2. Materials and methods

2.1. Immunization

Six-week-old BALB/c female mice were immunized with rhPIV2–Ag85B or rhPIV2 control vector 3 or 4 times at 2-week intervals by intranasal inoculation of 1×10^8 TCID50 virus in 20 μl PBS. Another group of mice was intramuscularly immunized twice with Ag85B DNA vaccine [11] and intranasally immunized twice with rhPIV2–Ag85B. As a control group, a group of mice was vaccinated using 1×10^7 CFU of BCG Tokyo by subcutaneous injection.

2.2. Infection assay

Two weeks (rhPIV2–Ag85B-immunized mice) or 6 weeks (BCG-immunized mice) after the final immunization, mice were challenged with *M. tuberculosis* (Mtb) Kurono strain by inhalation. This bacterial preparation and infection assay were performed as previously described [12]. In brief, the mice were infected *via* the airborne route by placing them into the exposure chamber of a Glas-Col aerosol generator. The nebulizer compartment was filled with 5 ml of a suspension containing 10^6 CFU of Kurono strain so that approximately 50 bacteria would be deposited in the lungs of each animal. Eight weeks after Mtb infection, mice were sacrificed and the preventive effects of the vaccine were assessed.

2.3. Cell culture

Human bronchial epithelial cells (BEAS cells) and primary cultured normal human bronchial epithelial (NHBE) cells were obtained from the American Type Culture Collection (Manassas, VA) and Lonza (Walkersville, MD). These cells were grown in bronchial epithelial growth medium containing supplements (Lonza). These cells were infected with rhPIV2 or rhPIV2–Ag85B (MOI of 10) or treated with recombinant Ag85B (10 μg/ml) for 6–48 h in a 37 °C incubator with a 5% CO_2 atmosphere.

2.4. FACS analysis

Spleen, pulmonary lymph node (pLN), and bronchoalveolar lavage (BAL) cells were obtained from immunized mice, and single-cell suspensions were prepared. The cells were incubated with recombinant Ag85B protein (10 μg/ml final concentration) for 4 h in the presence of Brefeldin A at 37 °C with 5% CO_2. The cells were stained for surface markers with anti-CD3 and anti-CD4 (BD Biosciences, San Joes, CA) for 30 min at 4 °C, followed by fixation for 30 min at 4 °C in 2% paraformaldehyde. IFN-γ was detected by staining with anti-IFN-γ (BD Biosciences) for 30 min at 4 °C. Flow cytometry data collection was performed on a FACS Canto II (BD Biosciences). Files were analyzed using FACSDiva Software (BD Biosciences). BEAS cells infected with rhPIV2–Ag85B were stained with anti-ICAM-1 (BioLegend, San Diego, CA) and analyzed as described above.

2.5. Evaluation of Ag85B-specific immune responses by ELISPOT assay

The number of Ag85B-specific, IFN-γ-secreting cells was determined by the ELISPOT assay according to the method reported previously [11]. Triplicate samples of whole, $CD4^+$, and $CD8^+$ T cells (separated by a MACS system) (Miltenyi Biotec, Bergisch Gladbach, Germany) collected from the spleen, pLN, and BAL were plated at 1×10^6 cells/well. These cells were stimulated by addition of 2×10^5 mitomycin C (Sigma–Aldrich, Saint Louis, MO)-treated syngeneic spleen cells infected with recombinant vaccinia virus expressing Ag85B or rhPIV2–Ag85B.

2.6. Statistical analysis

Data are presented as means ± SD. Statistical analyses were performed using the Mann–Whitney *U* test. Statistically significant differences compared with the control are indicated by asterisks.

3. Results

3.1. Characteristics of rhPIV2–Ag85B

A construction of rhPIV2–Ag85B is shown in Fig. 1A. To examine gene expression levels of the inserted Ag85B, BEAS cells were infected with rhPIV2–Ag85B. Abundant and rapid expression of mRNA of Ag85B was observed in BEAS cells infected with rhPIV2–Ag85B compared with the expression of NP mRNA (Fig. 1B). These results were also confirmed by analysis of protein expression (Fig. 1C). The production of Ag85B was earlier than that of NP, which is usually the earliest synthesized protein in hPIV2 infection.

inoculation ($n = 5$ per group). Spleen, pLN, and BAL cells were collected from immunized mice ($n = 5$ per group) 2 weeks after the final immunization for examination by an ELISPOT assay. These isolated cells were stimulated *in vitro* with syngeneic spleen cells infected with control rhPIV2, rhPIV2–Ag85B, or recombinant Ag85B protein (rAg85B) (10 μg/ml final concentration) for 24 h. Error bars represent standard deviations. Statistically significant differences are indicated by asterisks (*, $P < 0.05$ compared to the group stimulated with rhPIV2).

These responses were considered to be advantageous effects in cellular immune response to inserted Ag85B *versus* rhPIV2 vector. To confirm this advantageous response, cells from immunized mice were re-stimulated *in vitro* with syngeneic spleen cells infected with rhPIV2 or rhPIV2–Ag85B. Although responses to both Ag85B and rhPIV2 vector were observed, Ag85B-specific responses were clearly seen, especially in pLN and BAL cells after single immunization (Fig. 1D). After performing immunization twice, Ag85B-specific responses were also seen in spleen cells as booster effects more than responses to the vector virus (Fig. 1E). These results indicated that rhPIV2–Ag85B immunization elicited inserted Ag85B-specific immune responses without being hidden by vector responses.

3.2. Intranasal administration of rhPIV2–Ag85B prevents infection with Mtb in mice

To investigate the ability of intranasal administration of rhPIV2–Ag85B to elicit a protective effect against pulmonary TB, rhPIV2–Ag85B-immunized mice were aerosol-infected with highly pathogenic Mtb kurono strain [13]. One group of mice were intranasally immunized with rhPIV2–Ag85B 4 times at 2-week intervals, and another group of mice were intranasally immunized with rhPIV2–Ag85B twice following intramuscular immunization with Ag85B DNA twice (Fig. 2A). Intranasal administration of rhPIV2–Ag85B resulted in a decreases in granulomatous lesions and inflammatory area. However, there were no apparent histopathological differences, such as infiltrating cell types, between the each group of mice, and these results are similar to the results of another study focusing on TB vaccine [14]. On the other hand, these vaccine effects were clearly seen by staining for acid-fast bacillus. Mice immunized with rhPIV2–Ag85B showed a substantial reduction in the infiltration of bacteria, and this inhibitory effect on bacterial expansion was correlated with the number of rhPIV2–Ag85B intranasal administrations (Fig. 2B). CFU of Mtb in spleens from both groups of immunized mice was also significantly lower than those in mice immunized with the control vector (Fig. 2C). As for a preventive effect on Mtb infection in the lung, the mice immunized with rhPIV2–Ag85B clearly showed a substantial reduction in CFU.

3.3. Ag85B-specific immune response is elicited by rhPIV2–Ag85B administration

The capacity of rhPIV2–Ag85B intranasal immunization to elicit effector cells that recognize endogenously expressed Ag85B was assessed. Spleen, pLN, and BAL cells obtained from immunized mice were re-stimulated *in vitro* with syngeneic spleen cells infected with the recombinant vaccinia virus expressing Ag85B, and endogenously expressed Ag85B-specific cellular immune response was examined by ELISPOT assays. Both $CD4^+$ and $CD8^+$ splenocytes exhibited Ag85B-specific responses, and $CD8^+$ T cells showed much stronger responses than those of $CD4^+$ T cells in splenocytes from mice immunized with rhPIV2–Ag85B (Fig. 3A). Ag85B-specific responses were also seen in both $CD4^+$ and $CD8^+$ T cells at almost the same levels in pLN and BAL cells (Fig. 3B and C).

3.4. Analysis of Ag-specific effector cells and immune responses in pLN cells and the lung

Delayed initial activation of effector cells in lungs has been reported in the case of Mtb infection [15]. To control bacterial expansion in the early phase of infection, rapid Mtb Ag-specific $CD4^+$ T cell responses are required. Thus, we next analyzed recruitment of Ag85B-specific IFN-γ^+ $CD4^+$ T cells in pLN and BAL cells in mice immunized with rhPIV2–Ag85B. Mice were intranasally immunized with rhPIV2–Ag85B or the control vector virus 3 times

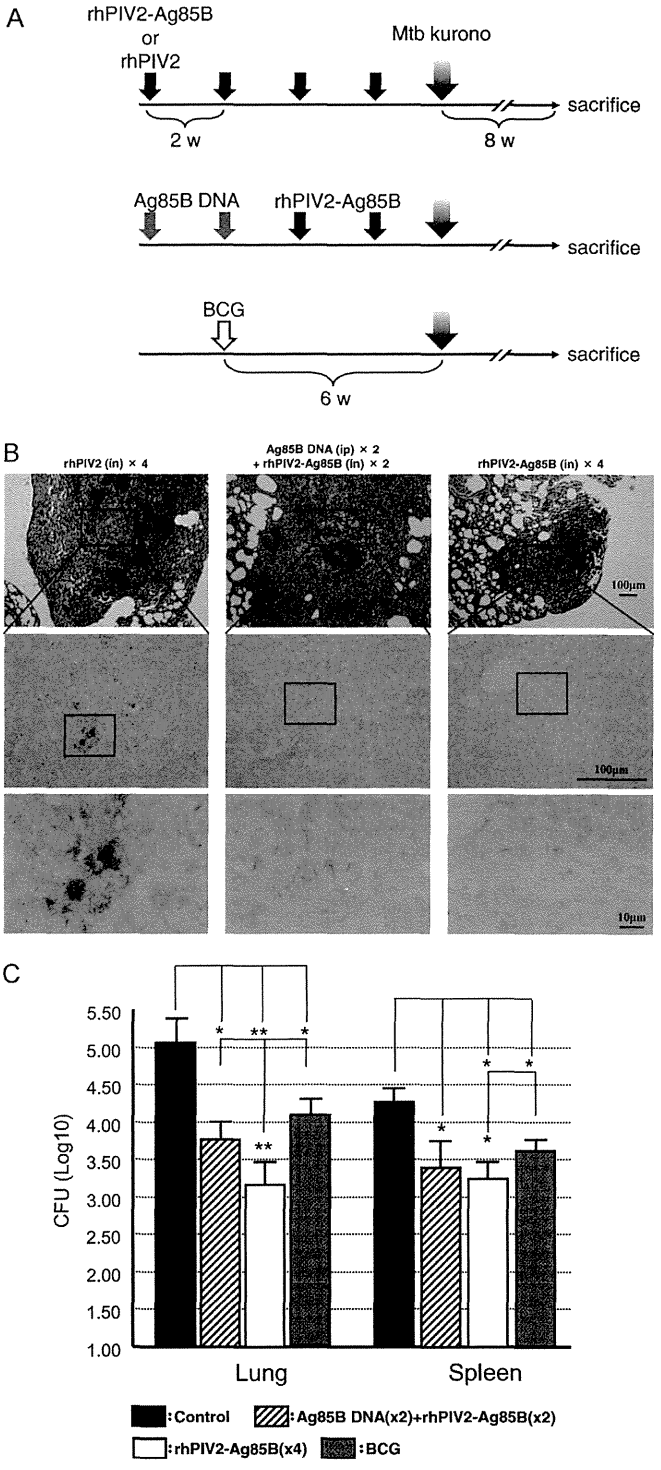

Fig. 2. Repeated immunization with rhPIV2–Ag85B results in protection from TB. (A) Groups of mice were vaccinated in this schedule. (B) Histological images of the lungs of Mtb-infected mice. Groups of mice ($n = 10$) immunized 4 times with rhPIV2 (left panel), 2 times with Ag85B DNA vaccine and 2 times with rhPIV2–Ag85B (middle panel) or 4 times with rhPIV2–Ag85B (right panel) were challenged by Mtb infection. Arrows point to tubercles. Lower panels in (B) show magnified images of images in the middle panels. (C) Inhibition of bacterial growth by immunization with rhPIV2–Ag85B in the lung and spleen. Groups of mice immunized 2 times with Ag85B DNA vaccine and 2 times with rhPIV2–Ag85B or immunized 4 times with rhPIV2–Ag85B or BCG were challenged by Mtb infection. The numbers of Mtb CFU in the lung and spleen were determined by a colony enumeration assay. The bacterial load is represented as mean $\log_{10}$ CFU per organ. Error bars represent standard deviations. Statistically significant differences are indicated by asterisks (*, $P < 0.05$, **, $P < 0.005$).

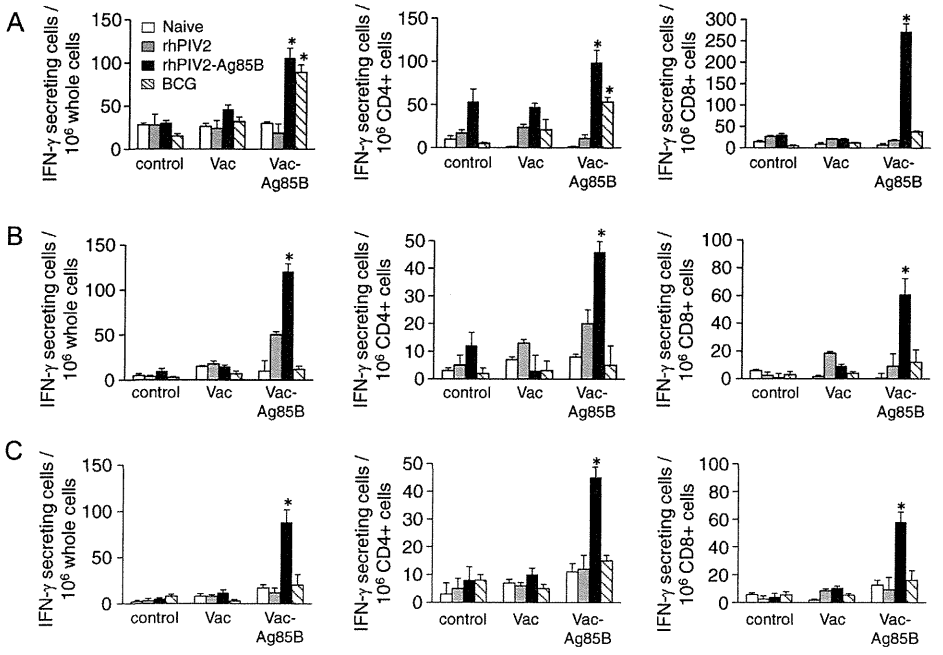

Fig. 3. Induction of Ag85B-specific cellular immune responses in rhPIV2–Ag85B-immunized mice. Mice were immunized with rhPIV2, rhPIV2–Ag85B, or BCG ($n = 5$ per group) according to the schedule shown in Fig. 2A. Two (rhPIV2 or rhPIV2–Ag85B) or 4 weeks (BCG) after the final immunization, the spleen, pLN, and BAL were collected. Isolated cells from the spleen (A), pLN (B), or BAL (C) were separated into whole (left panels), $CD4^+$ (middle panels), and $CD8^+$ (right panels) T cells and examined for IFN-γ production in an ELISPOT assay. These cells were stimulated *in vitro* with syngeneic spleen cells infected with control vaccinia virus (Vac) or recombinant vaccinia virus carrying the Ag85B gene (Vac-Ag85B) for 24 h. Error bars represent standard deviations. Statistically significant differences are indicated by asterisks (*, $P < 0.01$ compared to the group stimulated with Vac).

at 2-week intervals. Another group of mice were immunized with BCG by subcutaneous injection. Two weeks (rhPIV2–Ag85B-immunized mice) or 6 weeks (BCG-immunized mice) after the final immunization, all mice were challenged with Mtb Kurono strain by inhalation (Fig. 4A). At each time point after immunization or Mtb challenge, the percentage and absolute number of Ag85B-specific IFN-γ^+ $CD4^+$ cells were determined by flow cytometry. Before Mtb challenge, the percentage of IFN-γ^+ $CD4^+$ cells in pLN cells was increased by immunization with rhPIV2–Ag85B but not by BCG immunization (Fig. 4B and C, top). However, a significant increase in IFN-γ^+ $CD4^+$ cells was not detected in BAL cells (Fig. 4B and C, bottom). Interestingly, expansion of IFN-γ^+ $CD4^+$ cells occurred after Mtb challenge in BAL cells more dramatically than that in pLN cells in terms of absolute number (Fig. 4C). These responses induced by rhPIV2–Ag85B immunization were much stronger than those induced by BCG immunization.

Similarly, an increase in Ag85B-specific responses was observed by the ELISPOT assay (Fig. 4D). The number of Ag85B-specific IFN-γ secreting cells increased in pLN cells from mice immunized with rhPIV2–Ag85B in a number of immunizations-dependent manner. Furthermore, strong Ag85B-specific responses were detected after Mtb challenge in pLN and BAL cells, and the responses were much stronger than those in BCG immunized mice.

3.5. *rhPIV2–Ag85B induces innate immune responses*

We explored innate immune responses induced by rhPIV2–Ag85B infection. We confirmed that Ag85B did not affect the viability of rhPIV2–Ag85B infected cells (Supplemental Fig. 1) [44–46]. Type I IFNs were assessed after infection with rhPIV2–Ag85B in NHBE and BEAS cells as an indication of innate immune responses. Both types of cells showed mRNA expression of type I IFNs after infection with rhPIV2–Ag85B but not after addition of recombinant Ag85B protein (Fig. 5A). Production of IFN-β was also detected in the culture supernatant by ELISA (Fig. 5B). The mRNA expression of intracellular receptors, RIG-I, MDA5, and TLR3, and the induction of cytokines, IL-6 and IL-15 were also enhanced by infection with rhPIV2–Ag85B, whereas these effects were not observed with the addition of recombinant Ag85B protein (Fig. 5C and D). Furthermore, the expression of ICAM-1 was induced by infection with rhPIV2–Ag85B (Fig. 5E). Similar results were obtained after infection with rhPIV2 vector alone or rhPIV2-GFP (Supplemental Fig. 2). Other co-stimulation molecules, CD80, CD86, ICAM-2 and selectin, were not detected (data not shown).

To further investigate the participation of these receptors in innate immune activation induced by rhPIV2–Ag85B infection, expression of these receptors was knocked down by transfecting siRNA. At 48 h after transfection with siRNA, expression levels of these receptors were reduced by approximately 90% or expression was no longer detectable (Fig. 5F). IFN-β production induced by rhPIV2–Ag85B infection was inhibited when the cells were treated with RIG-I siRNA. For other receptors, MDA5 and TLR3, siRNA treatment did not result in inhibition of IFN-β production induced by rhPIV2–Ag85B infection (Fig. 5G). This result was confirmed by phosphorylation of IRF3, which is a downstream molecule of RIG-I in epithelial cells. The phosphorylation of IRF3 induced by rhPIV2–Ag85B infection was inhibited when epithelial cells were treated with siRNA of RIG-I (Fig. 5H).

4. Discussion

In the present study, we demonstrated the effectiveness of hPIV2 vectors for TB vaccines to induce systemic and mucosal immune responses. The rhPIV2 vector is a weak immunogenic; however, intranasal immunization with rhPIV2–Ag85B showed more potent protection against pulmonary TB in BALB/c mice than did conventional BCG vaccination. The rhPIV2–Ag85B shows a vaccine effect by itself alone, and this effect is more useful than the effects of other vectors for TB vaccines.

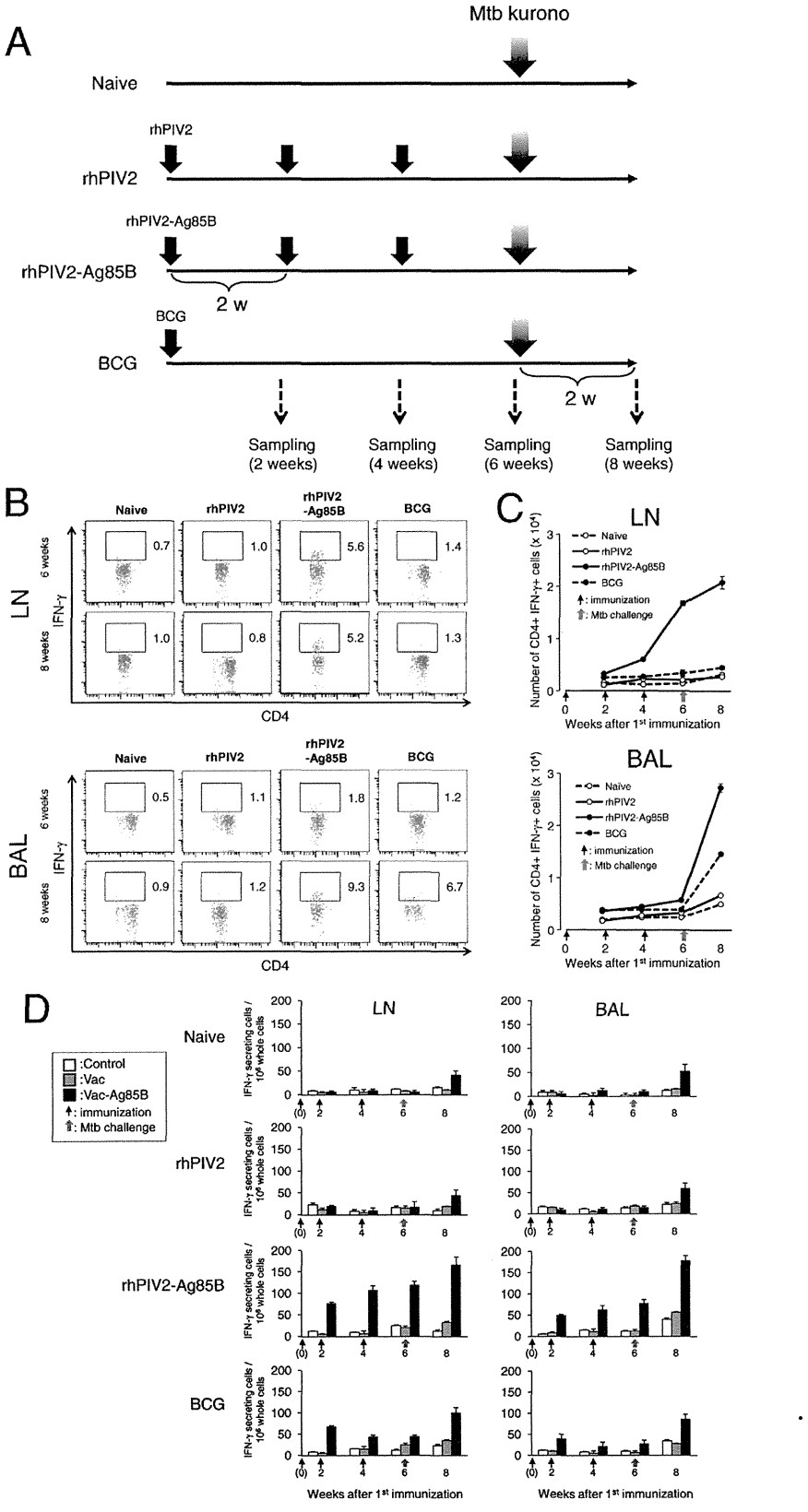

Fig. 4. Analysis of Ag-specific effector cells and these immune responses in pLN and BAL. (A) Groups of mice were immunized with rhPIV2, rhPIV2–Ag85B, or BCG ($n = 10$ per group) and challenged by Mtb infection in this schedule. (B) Representative flow cytometry plots of IFN-γ^+ cells on gated CD4$^+$ cells from pLN (top panels) and BAL (bottom panels) are shown. Numbers shown beside the gates represent the percentages within CD4$^+$ T cells. (C) Kinetics of recruitment of Ag85B-specific IFN-γ^+ cells in pLN (top panel) and BAL (bottom panel). Absolute numbers of IFN-γ^+ CD4$^+$ cell populations at each time points are shown. Error bars represent standard deviations. (D) Isolated cells from the pLN and BAL at each time point were examined for IFN-γ production in an ELISPOT assay. These cells were stimulated *in vitro* with syngeneic spleen cells infected with control vaccinia virus (Vac) or recombinant vaccinia virus carrying the Ag85B gene (Vac-Ag85B) for 24 h. Error bars represent standard deviations.

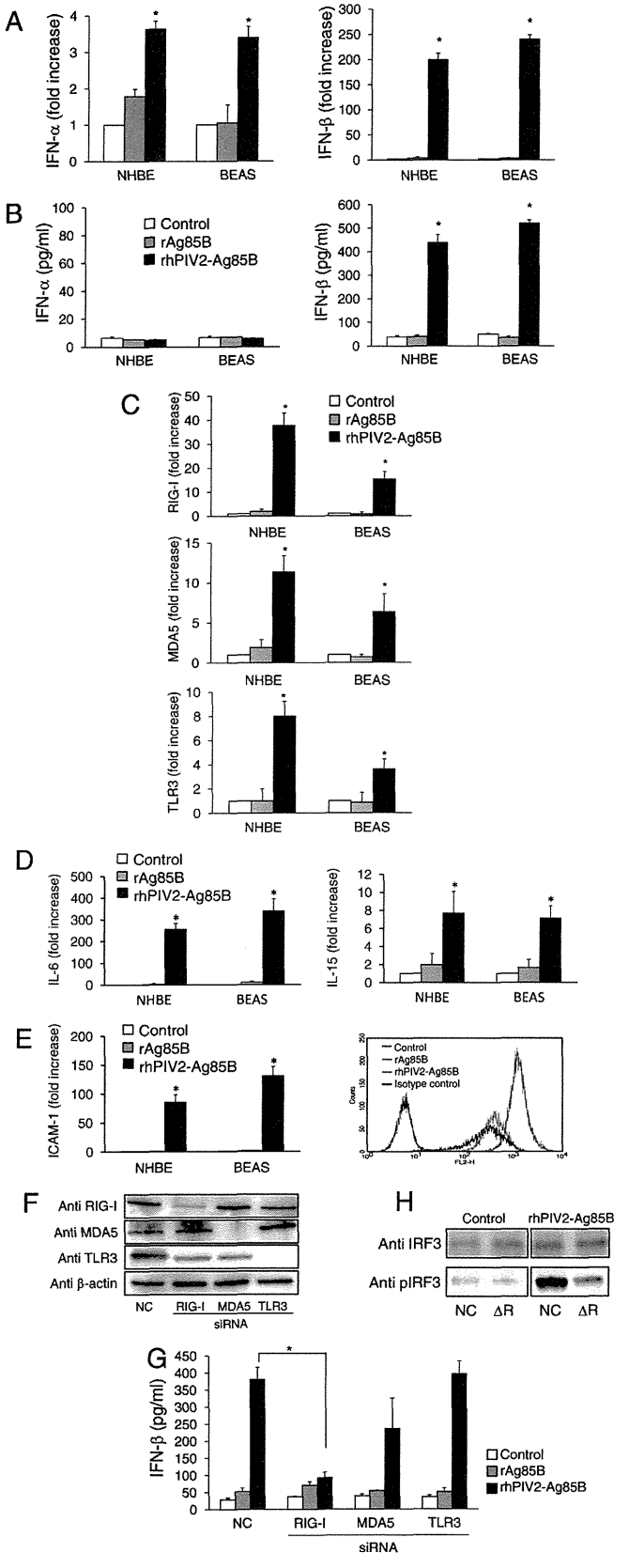

Fig. 5. Evaluation of adjuvant activity of rhPIV2–Ag85B *in vitro*. NHBE and BEAS cells were treated with rAg85B protein (10 μg/ml) or infected with rhPIV2–Ag85B (MOI of 10) for 24 h, and the increases in mRNA levels of IFN-α, IFN-β (A), RIG-I, MDA5, TLR3 (C), IL-6, IL-15 (D), and ICAM-1 (E, left panel) were determined by real-time PCR. Fold increase of each target gene was normalized to β-actin, and the expression levels are represented as relative values to the control. Culture supernatants were also collected, and amounts of secreted IFN-α and IFN-β were measured by ELISA (B). Expression of ICAM-1 was also confirmed by FACS analysis in BEAS cells (E, right panel). Data are averages of triplicate samples from three identical experiments, and error bars represent standard deviations. Statistically significant differences between control cells and rhPIV2–Ag85B-infected cells are indicated by asterisks (*, $P < 0.01$). BEAS cells were treated with siRNA targeting RIG-I, MDA5, TLR3, or the negative control siRNA (NC) for 48 h. Depletion of them was examined by immunoblotting (F). Those cells were stimulated by rAg85B protein (10 μg/ml) or infected with rhPIV2–Ag85B (MOI of 10) and then production of IFN-β was measured by ELISA (G). Data are averages of triplicate samples from three identical experiments, and error bars represent standard deviations. Statistically significant differences are indicated by asterisks (*, $P < 0.01$ compared to NC). The effects of depletion of RIG-I on IRF3 phosphorylation were tested. BEAS cells treated with NC or siRNA targeting RIG-I (Δ*R*) for 48 h were infected with rhPIV2–Ag85B or not infected (control). Whole IRF3 and phosphorylated IRF3 (pIRF3) were detected by immunoblotting 6 h after infection (H).

Viral vectors are promising vaccine candidates for eliciting Ag-specific immune responses [16,17]. Pre-existing anti-vector antibodies, however, constitute an obstacle for use in humans [18–20]. Although antibodies against hPIV are known to cross-react with Sendai virus, Sendai virus vector is considered to be effective for human use by intranasal administration [21]. Additionally, Sendai virus vector is not affected by antibodies against Sendai virus for induction of T cell responses, especially when it is administered intranasally [4]. From these findings, intranasal administration of the hPIV2 vector is also considered to be effective for human use. In fact, multiple administrations with rhPIV2–Ag85B also showed preventive effects more clearly than did immunization 2 times with rhPIV2–Ag85B (Fig. 2).

Many viral vectors have been tested as recombinant viral vaccines eliciting suitable recombinant Ag-specific immune responses, and many of these vaccine vectors are not vaccine viruses such as vaccinia virus Ankara (MVA), adenovirus, Sendai virus, and CMV. These viral vectors have also been used in several vaccine trials in TB or HIV vaccine [22–24]. Experience in the HIV vaccine field has emphasized the importance of avoiding anti-vector immune responses when developing a vectored vaccine [25]. Immune responses to vaccine vectors prevent the induction of aimed immune responses against recombinant Ag. From these findings, elimination of the immunogenicity of a vaccine vector is critical for a recombinant viral vaccine. The immunogenicity of viral vectors depends on the amount of vector viral proteins. Approximately 80 poxvirus proteins are encoded by its over 130–300 kbp and the adenovirus genome sizes are 26–45 kbp. The genome sizes of these two viral vectors are much larger than that of hPIV2 (15.65 kbp), and induction of immune responses to hPIV2 vector might be lower than other viral vectors. In TB vaccines, recombinant vaccinia virus and adenovirus, which are immunogenic viruses, did not show clear vaccine effects against TB infection by immunization with themselves alone. These two recombinant TB vaccines, adenovirus and MVA, were utilized as boost immunization after BCG priming [26,27]. These heterologous prime-boost strategies diminish immune responses to the vector virus and indicate the possibility of a practical and efficient strategy for prevention of TB [28,29]. On the other hand, the most common method for obtaining an attenuated virus is gene elimination of the viral construct protein to make a replication-deficient virus *in vivo*. The rhPIV2 vector is a weak immunogenicity by elimination of structural protein (M) gene; however, the rhPIV2–Ag85B shows a vaccine effect by immunization with itself alone, and this effect is more useful than the effects of other vectors for a recombinant TB vaccine.

The hPIV2 vector has an additional advantage over other viral vectors. The inserted Ag85B gene, which is only 978 bp, is a minor component of rhPIV2–Ag85B. Despite that, the cellular immune response against Ag85B had an advantage over that against the virus vector in mice. This advantageous effect is thought to depend

on Ag85B expression mechanisms. The frequency with which viral RNA polymerase reinitiates the next mRNA at gene junctions is imperfect, and this leads to a gradient of mRNA abundance that decreases according to distance from the genome 3′ end [30]. Insertion of the Ag85B gene into the 3′ proximal first locus between the leader sequence and the NP gene results in the highest level of gene expression. Ag85B is transcribed earlier and more abundantly than other viral products (Fig. 1B and C). This property of rhPIV2–Ag85B leads to elicit stronger Ag85B-specific immune responses than vector-specific responses in our system (Fig. 1D and E), although recombinant virus vaccine immunization usually induces overwhelming viral-specific immune responses compared with an inserted gene product [31,32]. We also demonstrated that intranasal administration of the rhPIV2 vector had no adverse effects and provided sufficient immunogenicity and a sufficient vaccine effect against Mtb in mice. These results suggest that intranasal administration of rhPIV2–Ag85B does not cause functional failure as a vaccine by multiple administrations, and these features of the rhPIV2 vector are definitely advantages for clinical use.

Another major feature of rhPIV2–Ag85B is effective prevention of TB by intranasal administration. Vaccination in the respiratory tract may enhance protection against Mtb infection, since Mtb initially establishes infection on mucosal surfaces of the respiratory tract. Indeed, a number of recombinant TB vaccines have been developed and evaluated for respiratory mucosal immunization [33–35]. It is important to note that lack of Ag-specific effector cells persists even up to about 21 days after pulmonary Mtb infection caused by a bacterial component [15,36]. In the present study, the arrival of Ag-specific T cells was detected in lung and pLN by rhPIV2–Ag85B immunization, and this arrival of effector cells was recognized faster than BCG immunization after Mtb challenge (Fig. 4B and C). We were able to establish a novel intranasal vaccine, rhPIV2–Ag85B, against TB by utilizing various advantages of intranasal administration. Nasal administration of a vaccine to induce mucosal and systemic immune responses has several advantages other than the induction of effective immune responses. It is even possible that intranasal administration of replication-incompetent rhPIV2–Ag85B limits the areas of infection in respiratory organs and induces a respiratory tract mucosal immune response in addition to a systemic immune response against TB. Our study suggested that intranasal administration of rhPIV2–Ag85B, which can induce both mucosal and systemic immune responses against Mtb, has a great advantage as a TB vaccine.

Attempts have been made to use various types of adjuvants for enhancing an immune responses to vaccines, including vaccines against TB [37]. In fact, a protein-based TB vaccine required the addition of an adjuvant to induce effective immune responses [38–41]. For the generation of adaptive immune responses, induction of innate immunity is crucial for vaccines to elicit potent Ag-specific immune responses. Pattern recognition receptors have been studied as potential targets for an adjuvant. dsRNA is a dominant activator of innate immunity because viral dsRNA is recognized by TLR3, RIG-I, and MDA5 [42,43]. As a result, it was demonstrated that the rhPIV2 vector had a potent adjuvant activity as dsRNA recognized by the RIG-I receptor and enhanced not only local innate immunity but also systemic adaptive immunity. It is possible that no extra addition of an adjuvant is required to prevent TB by vaccination with rhPIV2–Ag85B. Furthermore, the inhibitory effects on the growth of rhPIV2–Ag85B *in vivo* by IFN through the innate receptor are not required to consider since the rhPIV2 vector is replication-incompetent *in vivo* by elimination of the M gene (Fig. 1A).

In summary, our results provide evidence for the possibility of rhPIV2–Ag85B as a novel intranasal vaccine for eliciting Mtb-specific mucosal immunity. Immunization with rhPIV2–Ag85B showed significant protection against TB without any prime vaccine or addition of an adjuvant in mice. Further studies will contribute to the ultimate goal of establishing a new vaccine strategy that can definitely prevent Mtb infection.

Acknowledgements

We thank members of AERAS for helpful advice and Dr. Yasuhiko Ito (Chubu University, Japan) and Dr. Isamu Sugawara (The Research Institute of Tuberculosis) for useful suggestion. This work was supported by Health Science Research Grants from the Ministry of Health, Labor and Welfare of Japan and the Ministry of Education, Culture, Sports, Science and Technology of Japan. This work was also supported by a grant from the Cooperative Link of Unique Science and Technology for Economy Revitalization (CLUSTER) promoted by the Ministry of Education, Culture, Sports and Technology, Japan.

Appendix A. Supplementary data

Supplementary material related to this article can be found, in the online version, at http://dx.doi.org/10.1016/j.vaccine.2013.11.108.

References

[1] Small JC, Ertl HC. Viruses – from pathogens to vaccine carriers. Curr Opin Virol 2011;1(October (4)):241–5.
[2] Halle S, Dujardin HC, Bakocevic N, Fleige H, Danzer H, Willenzon S, et al. Induced bronchus-associated lymphoid tissue serves as a general priming site for T cells and is maintained by dendritic cells. J Exp Med 2009;206(November (12)):2593–601.
[3] Okano S, Yonemitsu Y, Shirabe K, Kakeji Y, Maehara Y, Harada M, et al. Provision of continuous maturation signaling to dendritic cells by RIG-I-stimulating cytosolic RNA synthesis of Sendai virus. J Immunol 2011;186(February (3)):1828–39.
[4] Moriya C, Horiba S, Kurihara K, Kamada T, Takahara Y, Inoue M, et al. Intranasal Sendai viral vector vaccination is more immunogenic than intramuscular under pre-existing anti-vector antibodies. Vaccine 2011;29(November (47)):8557–63.
[5] Randomised controlled trial of single BCG, repeated BCG, or combined BCG and killed *Mycobacterium leprae* vaccine for prevention of leprosy and tuberculosis in Malawi. Karonga Prevention Trial Group. Lancet 1996;348(July (9019)):17–24.
[6] Rodrigues LC, Pereira SM, Cunha SS, Genser B, Ichihara MY, de Brito SC, et al. Effect of BCG revaccination on incidence of tuberculosis in school-aged children in Brazil: the BCG-REVAC cluster-randomised trial. Lancet 2005;366(October (9493)):1290–5.
[7] Zinselmeyer BH, Dempster J, Gurney AM, Wokosin D, Miller M, Ho H, et al. In situ characterization of CD4+ T cell behavior in mucosal and systemic lymphoid tissues during the induction of oral priming and tolerance. J Exp Med 2005;201(June (11)):1815–23.
[8] Dwivedy A, Aich P. Importance of innate mucosal immunity and the promises it holds. Int J Gen Med 2011;4:299–311.
[9] Kiyono H, Kweon MN, Hiroi T, Takahashi I. The mucosal immune system: from specialized immune defense to inflammation and allergy. Acta Odontol Scand 2001;59(June (3)):145–53.
[10] Kawano M, Kaito M, Kozuka Y, Komada H, Noda N, Nanba K, et al. Recovery of infectious human parainfluenza type 2 virus from cDNA clones and properties of the defective virus without V-specific cysteine-rich domain. Virology 2001;284(May (1)):99–112.
[11] Takamura S, Matsuo K, Takebe Y, Yasutomi Y. Ag85B of mycobacteria elicits effective CTL responses through activation of robust Th1 immunity as a novel adjuvant in DNA vaccine. J Immunol 2005;175(August (4)):2541–7.
[12] Sugawara I, Mizuno S, Yamada H, Matsumoto M, Akira S. Disruption of nuclear factor-interleukin-6, a transcription factor, results in severe mycobacterial infection. Am J Pathol 2001;158(February (2)):361–6.
[13] Sugawara I, Yamada H, Kazumi Y, Doi N, Otomo K, Aoki T, et al. Induction of granulomas in interferon-gamma gene-disrupted mice by avirulent but not by virulent strains of *Mycobacterium tuberculosis*. J Med Microbiol 1998;47(October (10)):871–7.
[14] Sweeney KA, Dao DN, Goldberg MF, Hsu T, Venkataswamy MM, Henao-Tamayo M, et al. A recombinant *Mycobacterium smegmatis* induces potent bactericidal immunity against *Mycobacterium tuberculosis*. Nat Med 2011;17(October (10)):1261–8.

[15] Shafiani S, Tucker-Heard G, Kariyone A, Takatsu K, Urdahl KB. Pathogen-specific regulatory T cells delay the arrival of effector T cells in the lung during early tuberculosis. J Exp Med 2010;207(July (7)):1409–20.
[16] Draper SJ, Heeney JL. Viruses as vaccine vectors for infectious diseases and cancer. Nat Rev Microbiol 2010;8(January (1)):62–73.
[17] Clark KR, Johnson PR. Gene delivery of vaccines for infectious disease. Curr Opin Mol Ther 2001;3(August (4)):375–84.
[18] Sumida SM, Truitt DM, Lemckert AA, Vogels R, Custers JH, Addo MM, et al. Neutralizing antibodies to adenovirus serotype 5 vaccine vectors are directed primarily against the adenovirus hexon protein. J Immunol 2005;174(June (11)):7179–85.
[19] Catanzaro AT, Koup RA, Roederer M, Bailer RT, Enama ME, Moodie Z, et al. Phase 1 safety and immunogenicity evaluation of a multiclade HIV-1 candidate vaccine delivered by a replication-defective recombinant adenovirus vector. J Infect Dis 2006;194(December (12)):1638–49.
[20] Priddy FH, Brown D, Kublin J, Monahan K, Wright DP, Lalezari J, et al. Safety and immunogenicity of a replication-incompetent adenovirus type 5 HIV-1 clade B gag/pol/nef vaccine in healthy adults. Clin Infect Dis 2008;46(June (11)):1769–81.
[21] Hara H, Hironaka T, Inoue M, Iida A, Shu T, Hasegawa M, et al. Prevalence of specific neutralizing antibodies against Sendai virus in populations from different geographic areas: implications for AIDS vaccine development using Sendai virus vectors. Hum Vaccin 2011;7(June (6)):639–45.
[22] McShane H, Brookes R, Gilbert SC, Hill AV. Enhanced immunogenicity of CD4(+) t-cell responses and protective efficacy of a DNA-modified vaccinia virus Ankara prime-boost vaccination regimen for murine tuberculosis. Infect Immun 2001;69(February (2)):681–6.
[23] Radosevic K, Wieland CW, Rodriguez A, Weverling GJ, Mintardjo R, Gillissen G, et al. Protective immune responses to a recombinant adenovirus type 35 tuberculosis vaccine in two mouse strains: CD4 and CD8 T-cell epitope mapping and role of gamma interferon. Infect Immun 2007;75(August (8)):4105–15.
[24] Munier CM, Andersen CR, Kelleher AD. HIV vaccines: progress to date. Drugs 2011;71(March (4)):387–414.
[25] Cheng C, Wang L, Gall JG, Nason M, Schwartz RM, McElrath MJ, et al. Decreased pre-existing Ad5 capsid and Ad35 neutralizing antibodies increase HIV-1 infection risk in the Step trial independent of vaccination. PLoS ONE 2012;7(4):e33969.
[26] Abel B, Tameris M, Mansoor N, Gelderbloem S, Hughes J, Abrahams D, et al. The novel tuberculosis vaccine, AERAS-402, induces robust and polyfunctional CD4+ and CD8+ T cells in adults. Am J Respir Crit Care Med 2010;181(June (12)):1407–17.
[27] McShane H, Pathan AA, Sander CR, Keating SM, Gilbert SC, Huygen K, et al. Recombinant modified vaccinia virus Ankara expressing antigen 85A boosts BCG-primed and naturally acquired antimycobacterial immunity in humans. Nat Med 2004;10(November (11)):1240–4.
[28] Rahman S, Magalhaes I, Rahman J, Ahmed RK, Sizemore DR, Scanga CA, et al. Prime-boost vaccination with rBCG/rAd35 enhances CD8(+) cytolytic T-cell responses in lesions from *Mycobacterium tuberculosis*-infected primates. Mol Med 2012;18:647–58.
[29] Pathan AA, Minassian AM, Sander CR, Rowland R, Porter DW, Poulton ID, et al. Effect of vaccine dose on the safety and immunogenicity of a candidate TB vaccine, MVA85A, in BCG vaccinated UK adults. Vaccine 2012;30(August (38)):5616–24.
[30] Tokusumi T, Iida A, Hirata T, Kato A, Nagai Y, Hasegawa M. Recombinant Sendai viruses expressing different levels of a foreign reporter gene. Virus Res 2002;86(June (1–2)):33–8.
[31] Sakurai H, Kawabata K, Sakurai F, Nakagawa S, Mizuguchi H. Innate immune response induced by gene delivery vectors. Int J Pharm 2008;354(April (1–2)):9–15.
[32] Chen D, Murphy B, Sung R, Bromberg JS. Adaptive and innate immune responses to gene transfer vectors: role of cytokines and chemokines in vector function. Gene Ther 2003;10(June (11)):991–8.
[33] Wang J, Thorson L, Stokes RW, Santosuosso M, Huygen K, Zganiacz A, et al. Single mucosal, but not parenteral, immunization with recombinant adenoviral-based vaccine provides potent protection from pulmonary tuberculosis. J Immunol 2004;173(November (10)):6357–65.
[34] Dietrich J, Andersen C, Rappuoli R, Doherty TM, Jensen CG, Andersen P. Mucosal administration of Ag85B-ESAT-6 protects against infection with *Mycobacterium tuberculosis* and boosts prior bacillus Calmette-Guerin immunity. J Immunol 2006;177(November (9)):6353–60.
[35] Ballester M, Nembrini C, Dhar N, de Titta A, de Piano C, Pasquier M, et al. Nanoparticle conjugation and pulmonary delivery enhance the protective efficacy of Ag85B and CpG against tuberculosis. Vaccine 2011;29(September (40)):6959–66.
[36] Wolf AJ, Desvignes L, Linas B, Banaiee N, Tamura T, Takatsu K, et al. Initiation of the adaptive immune response to *Mycobacterium tuberculosis* depends on antigen production in the local lymph node, not the lungs. J Exp Med 2008;205(January (1)):105–15.
[37] Moreno-Mendieta SA, Rocha-Zavaleta L, Rodriguez-Sanoja R. Adjuvants in tuberculosis vaccine development. FEMS Immunol Med Microbiol 2010;58(February (1)):75–84.
[38] Lin PL, Dietrich J, Tan E, Abalos RM, Burgos J, Bigbee C, et al. The multistage vaccine H56 boosts the effects of BCG to protect cynomolgus macaques against active tuberculosis and reactivation of latent *Mycobacterium tuberculosis* infection. J Clin Invest 2012;122(January (1)):303–14.
[39] Aagaard C, Hoang T, Dietrich J, Cardona PJ, Izzo A, Dolganov G, et al. A multistage tuberculosis vaccine that confers efficient protection before and after exposure. Nat Med 2011;17(February (2)):189–94.
[40] Bertholet S, Ireton GC, Ordway DJ, Windish HP, Pine SO, Kahn M, et al. A defined tuberculosis vaccine candidate boosts BCG and protects against multidrug-resistant *Mycobacterium tuberculosis*. Sci Transl Med 2010;2(October (53)):53ra74.
[41] Von Eschen K, Morrison R, Braun M, Ofori-Anyinam O, De Kock E, Pavithran P, et al. The candidate tuberculosis vaccine Mtb72F/AS02A: tolerability and immunogenicity in humans. Hum Vaccine 2009;5(July (7)):475–82.
[42] Alexopoulou L, Holt AC, Medzhitov R, Flavell RA. Recognition of double-stranded RNA and activation of NF-kappaB by Toll-like receptor 3. Nature 2001;413(October (6857)):732–8.
[43] Kato H, Takeuchi O, Sato S, Yoneyama M, Yamamoto M, Matsui K, et al. Differential roles of MDA5 and RIG-I helicases in the recognition of RNA viruses. Nature 2006;441(May (7089)):101–5.
[44] Buchholz UJ, Finke S, Conzelmann KK. Generation of bovine respiratory syncytial virus (BRSV) from cDNA: BRSV NS2 is not essential for virus replication in tissue culture, and the human RSV leader region acts as a functional BRSV genome promoter. J Virol 1999;73(January (1)):251–9.
[45] Yasui F, Kai C, Kitabatake M, Inoue S, Yoneda M, Yokochi S, et al. Prior immunization with severe acute respiratory syndrome (SARS)-associated coronavirus (SARS-CoV) nucleocapsid protein causes severe pneumonia in mice infected with SARS-CoV. J Immunol 2008;181(November (9)):6337–48.
[46] Falkner FG, Moss B. *Escherichia coli* gpt gene provides dominant selection for vaccinia virus open reading frame expression vectors. J Virol 1988;62(June (6)):1849–54.

Nonagonistic Dectin-1 ligand transforms CpG into a multitask nanoparticulate TLR9 agonist

Kouji Kobiyama[a,b], Taiki Aoshi[a,b], Hirotaka Narita[c], Etsushi Kuroda[a,b], Masayuki Hayashi[a,b], Kohhei Tetsutani[a,b], Shohei Koyama[d,e], Shinichi Mochizuki[f], Kazuo Sakurai[f], Yuko Katakai[g], Yasuhiro Yasutomi[h], Shinobu Saijo[i,j], Yoichiro Iwakura[k], Shizuo Akira[l], Cevayir Coban[m], and Ken J. Ishii[a,b,1]

[a]Laboratory of Adjuvant Innovation, National Institute of Biomedical Innovation, Osaka 567-0085, Japan; Laboratories of [b]Vaccine Science, [l]Host Defense, and [m]Malaria Immunology, World Premier International Immunology Frontier Research Center and [c]Supramolecular Crystallography, Research Center for Structural and Functional Proteomics, Institute for Protein Research, Osaka University, Osaka 565-0871, Japan; [d]Department of Medical Oncology and [e]Cancer Vaccine Center, Dana-Farber Cancer Institute, Boston, MA 02115; [f]Department of Chemistry and Biochemistry, University of Kitakyushu, Fukuoka 808-0135, Japan; [g]Corporation for Production and Research of Laboratory Primates, Ibaraki 305-0843, Japan; [h]Tsukuba Primate Research Center, National Institute of Biomedical Innovation, Ibaraki 305-0843, Japan; [i]Department of Molecular Immunology, Medical Mycology Research Center, Chiba University, Chiba 260-8673, Japan; [j]Precursory Research for Embryonic Science and Technology, Japan Science and Technology Agency, Saitama 332-0012, Japan; and [k]Division of Experimental Animal Immunology, Research Institute for Biomedical Sciences, Tokyo University of Science, Chiba 278-8510, Japan

Edited by Rafi Ahmed, Emory University, Atlanta, GA, and approved January 16, 2014 (received for review October 12, 2013)

CpG DNA, a ligand for Toll-like receptor 9 (TLR9), has been one of the most promising immunotherapeutic agents. Although there are several types of potent humanized CpG oligodeoxynucleotide (ODN), developing "all-in-one" CpG ODNs activating both B cells and plasmacytoid dendritic cells forming a stable nanoparticle without aggregation has not been successful. In this study, we generated a novel nanoparticulate K CpG ODN (K3) wrapped by the nonagonistic Dectin-1 ligand schizophyllan (SPG), K3-SPG. In sharp contrast to K3 alone, K3-SPG stimulates human peripheral blood mononuclear cells to produce a large amount of both type I and type II IFN, targeting the same endosome where IFN-inducing D CpG ODN resides without losing its K-type activity. K3-SPG thus became a potent adjuvant for induction of both humoral and cellular immune responses, particularly CTL induction, to coadministered protein antigens without conjugation. Such potent adjuvant activity of K3-SPG is attributed to its nature of being a nanoparticle rather than targeting Dectin-1 by SPG, accumulating and activating antigen-bearing macrophages and dendritic cells in the draining lymph node. K3-SPG acting as an influenza vaccine adjuvant was demonstrated in vivo in both murine and nonhuman primate models. Taken together, K3-SPG may be useful for immunotherapeutic applications that require type I and type II IFN as well as CTL induction.

innate immunity | two-photon microscopy | MARCO | Siglec-1 | β-glucan

CpG oligodeoxynucleotide (CpG ODN) is a short (~20 bases), single-stranded synthetic DNA fragment containing the immunostimulatory CpG motif, a potent agonist for Toll-like receptor 9 (TLR9), which activates dendritic cells (DCs) and B cells to produce type I interferons (IFNs) and inflammatory cytokines (1, 2) and acts as an adjuvant toward both Th1-type humoral and cellular immune responses, including cytotoxic T-lymphocyte (CTL) responses (3, 4). Therefore, CpG ODN has been postulated as a possible immunotherapeutic agent against infectious diseases, cancer, asthma, and pollinosis (2, 5).

There are at least four types of CpG ODN, each of which has a different backbone, sequence, and immunostimulatory properties (6). D-type (also called A) CpG ODNs typically comprise one palindromic CpG motif with a phosphodiester (PO) backbone and phosphorothioate (PS) poly(G) tail, and activates plasmacytoid DCs (pDCs) to produce a large amount of IFN-α but fails to induce pDC maturation and B-cell activation (7, 8). The three other types of ODN consist of a PS backbone. K-type (also called B) CpG ODN contains nonpalindromic multiple CpG motifs, and strongly activates B cells to produce IL-6 and pDCs to maturation but barely produces IFN-α (8, 9). Recently, C and P CpG ODNs have been developed; these contain one and two palindromic CpG sequences, respectively, both of which can activate B cells like K-type and pDC like D-type, although C CpG ODN induces weaker IFN-α production compared with P CpG ODN (10–12).

D and P CpG ODNs have been shown to form higher-order structures, Hoogsteen base pairing to form parallel quadruplex structures called G tetrads, and Watson–Crick base pairing between *cis*- and *trans*-palindromic portions, respectively, that are required for robust IFN-α production by pDCs (12–14). Although such higher-order structures appear necessary for localization to early endosomes and signaling via TLR9, they suffer from product polymorphisms, aggregation, and precipitation, thereby hampering their clinical application (15). Therefore, only K and C CpG ODNs are generally available as immunotherapeutic agents and vaccine adjuvants for human use (16, 17). Although K CpG ODN enhances the immunogenicity of vaccines targeting infectious diseases and cancers in human clinical trials (6, 17), chemical or physical conjugation between antigen and K CpG ODN is necessary for optimal adjuvant effects. These results indicate that these four (K, D, P, and C) types of CpG ODN have advantages and disadvantages; however, the

Significance

CpG oligodeoxynucleotide (ODN), a Toll-like receptor 9 ligand, is a promising immunotherapeutic agent; however, developing an IFN-inducing CpG ODN forming a stable nanoparticle without aggregation has been unsuccessful. Here we generated a nanoparticulate CpG ODN (K3) wrapped by the nonagonistic Dectin-1 ligand schizophyllan (SPG), K3-SPG. K3-SPG stimulates human peripheral blood mononuclear cells to produce large amounts of both type I and II IFN. K3-SPG thus became a potent adjuvant, especially for cytotoxic T-lymphocyte (CTL) induction to coadministered protein antigens without conjugation, which is attributable to its nanoparticulate nature rather than to targeting Dectin-1. Protective potency of K3-SPG as an influenza vaccine adjuvant was demonstrated in both murine and nonhuman primate models. K3-SPG may be used as an IFN inducer as well as a CTL inducer for immunotherapeutic applications.

Author contributions: K.K., T.A., C.C., and K.J.I. designed research; K.K., T.A., H.N., M.H., and Y.K. performed research; T.A., H.N., E.K., M.H., K.T., S.M., K.S., Y.K., Y.Y., S.S., Y.I., and S.A. contributed new reagents/analytic tools; K.K., T.A., H.N., E.K., S.K., C.C., and K.J.I. analyzed data; and K.K., T.A., E.K., and K.J.I. wrote the paper.

Conflict of interest statement: K.S. holds a patent related to schizophyllan forming a complex with nucleic acids. K.K., T.A., and K.J.I. have filed a patent application related to the content of this manuscript.

This article is a PNAS Direct Submission.

Freely available online through the PNAS open access option.

[1]To whom correspondence should be addressed. E-mail: kenishii@biken.osaka-u.ac.jp.

This article contains supporting information online at www.pnas.org/lookup/suppl/doi:10.1073/pnas.1319268111/-/DCSupplemental.

development of an "all-in-one" CpG ODN activating both B cells and pDCs that forms a stable nanoparticle without aggregation has yet to be accomplished. A better strategy, targeting CpG ODN toward antigen-presenting cells (APCs), is desired to improve immunostimulatory specificity and immunotherapeutic efficacy of CpG ODNs.

Schizophyllan (SPG), a soluble β-glucan derived from *Schizophyllum commune*, is a drug that has been approved in Japan as an enhancer of radiotherapy in cervical carcinoma patients for the last three decades (18). It has been shown to form a complex with polydeoxyadenylic acid (dA) as a triple-helical structure (19). Although we previously demonstrated that mouse and humanized CpG ODN with PO poly(dA) at the 5′ end complexed with SPG enhanced cytokine production and acted as an influenza vaccine adjuvant (20, 21), it has been difficult to achieve high yields of the CpG–SPG complex toward its more efficient and cost-effective preclinical as well as clinical development. Recently, when the PS backbone of the dA sequence was linked to CpG ODN, the efficacy of complex formation was elevated by nearly 100% (22). However, a thorough investigation has yet to be conducted to identify the best humanized CpG sequence and optimization of factors to gain all-in-one activities of the four types of CpG ODN.

To do this, we sought to optimize a humanized CpG–SPG complex as a vaccine adjuvant and immunostimulatory agent in humans (in vitro), mice (in vitro and in vivo), and nonhuman primates (in vivo). In this study, we identified a novel K CpG ODN (K3) and SPG complex, namely K3-SPG. It forms a higher-order nanoparticle that can be completely solubilized. We found that this all-in-one K3-SPG displayed a more potent activity than, and different characteristics from, any other type of CpG ODN and previous CpG–SPG complexes.

Results

A Rod-Shaped Nano-Sized Particle of K3-SPG Gains Dual Characteristics of K- and D-Type CpG ODNs. To make a complex between CpG ODNs and schizophyllan (SPG), CpG ODNs need additional sequences of phosphorothioate backbone of 40-mer polydeoxyadenylic acid (dA_{40}) at the 5′ or 3′ end (20, 22). Fig. 1*A* shows methods of CpG ODN and SPG complexation through denaturing–renaturing procedures. In this study, we selected K3 as a K-type CpG ODN. At first, we examined the immunostimulatory impacts of the 5′ and 3′ ends of CpG ODN. 5′-K3-dA_{40}-3′, but not 5′-dA_{40}-K3-3′, complexed with SPG-activated human peripheral blood mononuclear cells (PBMCs) to produce a robust amount of IFN-α (Fig. 1*B* and Fig. S1). K3, K3-dA_{40}, or dA_{40}-K3, which are able to activate human PBMCs to produce other cytokines such as IL-6, failed to produce IFN-α (Fig. 1*B* and Fig. S1). These results indicate that the 5′-CpG sequence (K3-SPG) is more desirable than the 3′-CpG sequence as a novel TLR9 agonist. Although some CpG ODN-induced cytokine production is known to have a dose-dependent correlation, K3-SPG–induced IFN-α production is not. Given that previous reports showed that IFN-α pro-duction by K CpG ODN stimulation has a bell-shaped dose–response correlation (7), altogether these results suggest that K3-SPG still has the character of K CpG ODN.

Qualification and quantitation of K3-SPG were conducted by scanning electron microscopy (SEM) and dynamic light scattering (DLS). K3-SPG had a rod-like structure, consistent with that seen in a previous report (23) (Fig. 1*C*). It appeared to be a soluble monomeric nanoparticle with an average diameter of 30 nm, comparable to SPG itself and smaller than D CpG ODN (D35) (14, 24) (Fig. 1*D*). Given that K3-SPG forms a nanoparticle, we compared the immunostimulatory activities of K3-SPG with D, C, and P CpG ODNs. PBMCs stimulated with K3-SPG produced larger amounts of IFN-α and IFN-γ but at far lower concentrations than those induced by D35 (Fig. 1*E*) and P and C CpG ODNs (Fig. S2). These results suggest that K3-SPG gains the characteristic of D CpG ODN without losing that of the K type, because these IFNs are known to be D type-specific cytokines (7, 8, 25). To understand the dual functions of K and D

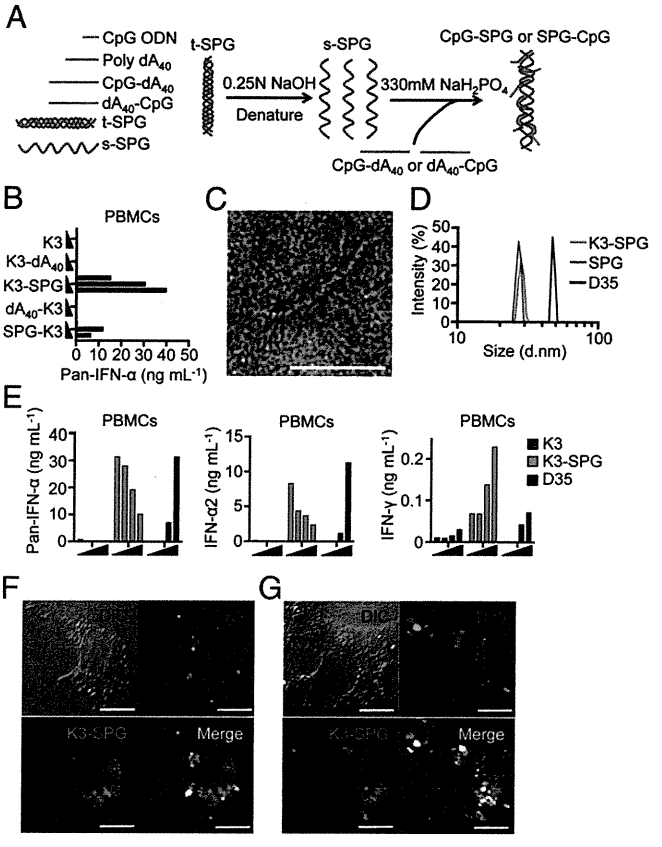

Fig. 1. K (B) CpG ODN and SPG complex forms nanoparticles and gains D (A) CpG ODN characteristics. (*A*) Methods of CpG ODN and SPG complexation. tSPG, triple-stranded SPG; sSPG, single-stranded SPG. (*B*) Production of IFN-α by human PBMCs stimulated with K3, K3-dA_{40}, K3-SPG, dA_{40}-K3, or SPG-K3 (adjusted for K3 ODN concentration at 0.1, 0.3, or 1 μM) for 24 h was measured by ELISA. (*C*) K3-SPG processed for SEM. (Scale bar, 50 μm.) (*D*) Size of K3-SPG, SPG, and D35 was analyzed by DLS. (*E*) Production of type I and II IFNs by PBMCs stimulated with K3, K3-SPG, or D35 for 24 h was measured by ELISA. (*F* and *G*) Mouse BMDMs were stimulated with Alexa 488-K3 (*F*) or Alexa 488-D35 (*G*) and Alexa 647-K3-SPG at 1 μM for 3 h. The cells were incubated with Hoechst 33258, fixed, and analyzed by fluorescence microscopy. DIC, differential interference contrast. (Scale bars, 10 μm.) Data represent one of three independent experiments with similar results.

CpG ODNs, we analyzed the intracellular localization of K3-SPG in bone marrow-derived macrophages (BMDMs). K3-SPG was colocalized with not only the endosomes containing K CpG ODN but also those containing D CpG ODN (Fig. 1 *F* and *G*) such as C CpG ODN (26), suggesting that K3-SPG may transduce endosome-mediated innate immune signaling pathways by K and D CpG ODNs. These results strongly suggest that K3-SPG forms a nano-sized higher-order and completely solubilized particle and found that this all-in-one K3-SPG displayed a more potent activity than, and different characteristic from, any other CpG ODNs and previously known CpG–SPG complex.

K3-SPG Is a Prominent Vaccine Adjuvant That Induces Potent CTL Responses to Protein Antigen Without Conjugation. We compared the adjuvant effects of K3, K3-dA_{40}, and K3-SPG in a murine immunization model. When wild-type mice were immunized with LPS-free chicken ovalbumin protein (OVA) alone or OVA with each K3-derived adjuvant, K3-SPG induced significantly higher humoral immune responses (Fig. 2*A*) and stronger T-cell responses than that induced by K3 (Fig. 2*B*). Of note, tetramer assays revealed a significantly greater number of OVA-specific CD8 T cells (Fig. 2*C*). We also observed very strong in vivo CTL activity against

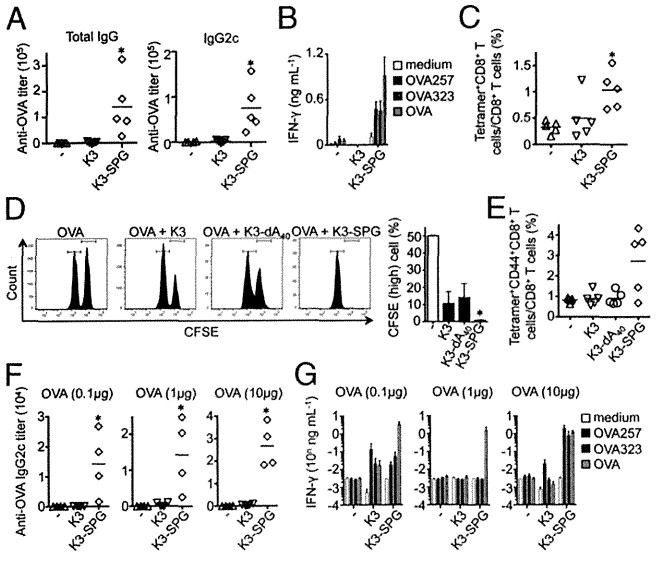

Fig. 2. K3-SPG acts as a potent vaccine adjuvant by simple mixture with antigen. Adjuvant activities of K3-SPG were analyzed. C57BL/6J mice (n = 4 or 5) were immunized s.c. with OVA protein antigen and various adjuvants. OVA-specific serum IgG (*A*), IFN-γ (*B*), and $OVA_{257-264}$-specific tetramer (*C*) were monitored (*d17*) after immunization (*d0* and *d10*) with OVA (100 μg) with or without K3 (10 μg) or K3-SPG (10 μg). (*D*) In vivo CTL assay 7 d after priming with OVA and various adjuvants as indicated. (*E*) Immunization with $OVA_{257-264}$ peptide (10 μg) with or without adjuvant as indicated. (*F* and *G*) Dose-sparing study; OVA-specific serum IgG and IFN-γ were monitored after immunization as in *A* and *B*. *$P < 0.05$ (Mann–Whitney U test). Data represent one of two or three independent experiments with similar results.

coadministered protein antigens lacking any covalent conjugation (Fig. 2*D*). This strong CTL induction by K3-SPG was reproduced by peptide vaccination (Fig. 2*E*) and was dose-dependent (Fig. S3). The antigen-sparing ability of K3-SPG was so potent that comparable antibody and CD4 T-cell responses were achieved using one-hundredth the amount of OVA antigen (Fig. 2 *F* and *G*). These results clearly indicate that K3-SPG is a more prominent adjuvant than K3 alone.

SPG Is a Soluble Dectin-1 Ligand but Is Not a Dectin-1 Agonist. We examined the role of Dectin-1 in cellular uptake of, and following activation by, SPG and K3-SPG, as Dectin-1 has been shown to be a receptor for β-glucans such as Zymosan (27). Using flow cytometry, we found that HEK293 cells expressing Dectin-1 but not Dectin-2 or a control (vector) increased the uptake of SPG or K3-SPG in vitro regardless of ODN presence (Fig. 3 *A* and *B*). It has recently been reported that the soluble form of β-glucan does not activate Dectin-1 signaling (28). Additionally, Dectin-1 signaling inhibits TLR9-mediated cytokine production through suppressor of cytokine signaling 1 induction (29). Therefore, we examined the agonistic activity of SPG. When splenocytes were stimulated with Zymosan-Depleted but not SPG, dose- and Dectin-1–dependent TNF-α and other cytokine production was observed, whereas cytokine production by Zymosan and Curdlan was Dectin-1–independent (Fig. 3*C* and Fig. S4). Zymosan-Depleted inhibited CpG ODN-induced IFN-α, with this inhibition relieved by Dectin-1 deficiency (Fig. 3*D*). In contrast, SPG did not inhibit CpG ODN-induced IFN-α production (Fig. 3*E*). These results indicate that SPG is a ligand but not an agonist of Dectin-1; therefore, SPG does not interfere with TLR9-mediated IFN-α production.

Adjuvant Effects of K3-SPG Are Dependent on TLR9 and Partially Dependent on Dectin-1. Because K3-SPG is a complex of CpG ODN and β-glucan, we examined the role of TLR9 (1) and Dectin-1 (30) using receptor knockout mice. When splenocytes and Flt3 ligand-induced bone marrow-derived DCs (FL-DCs) from *Tlr9*- and *Dectin-1*–deficient mice were stimulated with K3-SPG, cytokine production was completely dependent on TLR9 but not Dectin-1, excluding IL-12 p40 production (Fig. 4 *A–D*). K3-SPG–induced IL-12 p40 production showed two peaks, where the first peak of its production, but not the second peak at a higher dose, was dependent on Dectin-1 (Fig. 4*D*). This result may imply that Dectin-1 expression is involved in IL-12 p40 production at a lower dose of K3-SPG in vitro. Consistent with in vitro results, immunization of *Tlr9*-deficient mice with K3-SPG plus OVA resulted in diminished humoral and T-cell responses (Fig. 4 *E–G*). *Dectin-1*–deficient mice showed comparable immune responses with wild-type mice when the mice were immunized with OVA plus 10 μg of K3-SPG (Fig. S5). When *Dectin-1*–deficient mice were immunized with OVA plus 1 μg of K3-SPG, mice exhibited a reduced CD8 T-cell response according to the tetramer assays (Fig. 4*J*), with no significant changes in antibody and cytokine production from T cells (Fig. 4 *H* and *I*). These results suggest that the adjuvant effect of K3-SPG is dependent on TLR9 signaling. Although SPG and K3-SPG do not stimulate Dectin-1 signaling, the effect of K3-SPG is still partially dependent on Dectin-1 in vivo.

MARCO⁺, but Not Siglec-1⁺, Macrophages in Draining Lymph Nodes Dominantly Capture K3-SPG with Antigen. Given that K3-SPG provides potent adjuvant effects in vivo through immunization with a simple antigen mixture, we hypothesized that cells that capture both antigen and K3-SPG should play a critical role in mediating adjuvant effects. To examine in vivo distribution of fluorescence-labeled OVA and K3-SPG, we used fluorescence microscopy and two-photon microscopy. After an injection at the

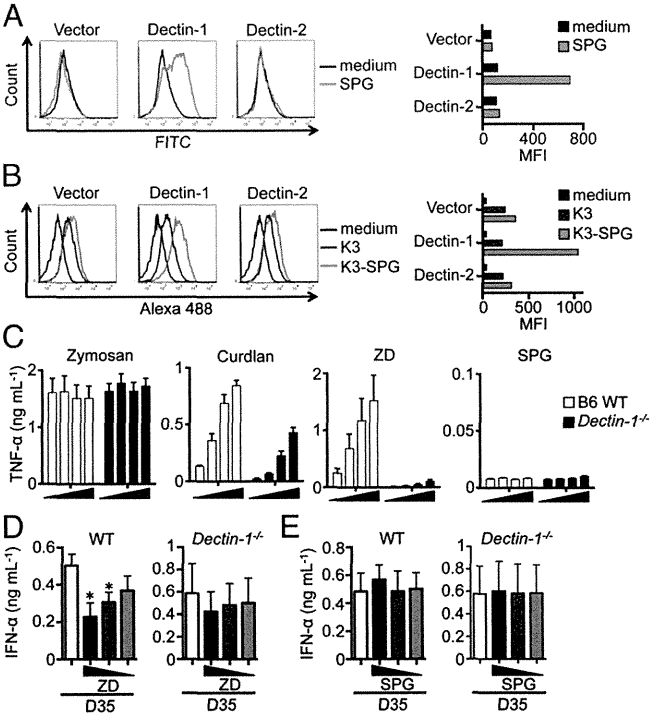

Fig. 3. SPG is a nonagonistic Dectin-1 ligand, but does not interfere with TLR9-mediated IFN-α production. (*A* and *B*) HEK293 cells transiently expressing Dectin-1 or Dectin-2 were treated with SPG-FITC (*A*), Alexa 488-K3, or Alexa 488-K3-SPG (*B*) for 60 min, and then their cellular uptake was monitored by flow cytometry [*Left*, histogram; *Right*, mean fluorescent intensity (MFI)]. Splenocytes from C57BL/6J and *Dectin-1*$^{-/-}$ mice (n = 3) were stimulated with Zymosan, Curdlan, Zymosan-Depleted (ZD), or SPG (3.7–100 μg/mL) (*C*), with D35 (1 μM), or with or without ZD (11.1–100 μg/mL) (*D*) or SPG (*E*) for 24 h and supernatant cytokines were monitored by ELISA. *$P < 0.05$ (t test). Data represent one of three independent experiments with similar results.